



**UNIVERSITY OF LEEDS**

This is a repository copy of *An eco-driving strategy for electric vehicle based on the powertrain.*

White Rose Research Online URL for this paper:

<https://eprints.whiterose.ac.uk/177239/>

Version: Accepted Version

---

**Article:**

Liao, P, Tang, T-Q, Liu, R [orcid.org/0000-0003-0627-3184](https://orcid.org/0000-0003-0627-3184) et al. (1 more author) (2021) An eco-driving strategy for electric vehicle based on the powertrain. *Applied Energy*, 302. 117583. ISSN 0306-2619

<https://doi.org/10.1016/j.apenergy.2021.117583>

---

© 2021 Elsevier Ltd. This manuscript version is made available under the CC-BY-NC-ND 4.0 license <http://creativecommons.org/licenses/by-nc-nd/4.0/>.

**Reuse**

This article is distributed under the terms of the Creative Commons Attribution-NonCommercial-NoDerivs (CC BY-NC-ND) licence. This licence only allows you to download this work and share it with others as long as you credit the authors, but you can't change the article in any way or use it commercially. More information and the full terms of the licence here: <https://creativecommons.org/licenses/>

**Takedown**

If you consider content in White Rose Research Online to be in breach of UK law, please notify us by emailing [eprints@whiterose.ac.uk](mailto:eprints@whiterose.ac.uk) including the URL of the record and the reason for the withdrawal request.



[eprints@whiterose.ac.uk](mailto:eprints@whiterose.ac.uk)  
<https://eprints.whiterose.ac.uk/>

[Click here to view linked References](#)

---

# An eco-driving strategy for electric vehicle based on the powertrain

Peng Liao<sup>a,b</sup>, Tie-Qiao Tang<sup>a\*</sup>, Ronghui Liu<sup>b</sup>, Hai-Jun Huang<sup>c</sup>

a) School of Transportation Science and Engineering, Beijing Key Laboratory for Cooperative Vehicle Infrastructure Systems and Safety Control, Beihang University, Beijing 100191, China

b) Institute for Transport Studies, University of Leeds, LS2 9JT, United Kingdom

c) School of Economics and Management, Beihang University, Beijing 100191, China

**Abstract:** Energy waste inside the powertrain of electric vehicles (EVs) due to non-optimized acceleration caused by the improper powertrain control variables is not generally considered when designing EVs' optimal driving strategies. To fill this gap, this study designs an optimal EV driving strategy taking a holistic approach by explicitly considering the powertrain's internal functionalities to minimize total energy consumption. Firstly, the battery thermal effect is introduced into the powertrain-based EV longitudinal dynamics model, aiming to improve the calculation accuracy of battery state of charge (SOC). Secondly, the eco-driving strategy for three basic driving modes is designed. Finally, the strategy feasibility is verified by its sensitivity to SOC and environment temperature, and its adaptability in realistic driving conditions is tested. Simulation results show that the extremely low SOC can drastically disturb the powertrain, causing acceleration and EV efficiency reduction up to 68.78% and 33.12% in the acceleration process, respectively. However, environment temperature has little effect on the powertrain. The required distance and time to complete the same speed-change task as NEDC are respectively reduced by 17.13% and 12.12%. The proportion of different driving modes in urban and suburban driving conditions is nearly consistent with the applicability preference of the corresponding strategies. The outcomes of this

---

\* Corresponding author: Tie-Qiao Tang (T.Q. Tang); email: [tieqiaotang@buaa.edu.cn](mailto:tieqiaotang@buaa.edu.cn)

---

study suggest that the proposed strategy can sufficiently utilize the powertrain coupling effect, and the EV energy consumption is limited by the battery degradation and the electromotor limitation.

**Keywords:** Eco-driving strategy; EV; powertrain; battery thermal effect; coupling effect

## 1. Introduction

Over the last decade, electric vehicles (EVs) have emerged rapidly as a powerful eco-friendly technology for the medium and long-term sustainable development goal [1]. However, the battery capacity with the current technology limits EVs' development, and minimizing the energy consumption of EVs becomes critical [2]. To this end, researchers have developed many eco-driving strategies to optimize the speed profile of EVs [3], taking into account of the external driving environment (e.g., road geometry, traffic conditions, regulations, and controls) and EV's dynamic capability (e.g., powertrain structure configuration, engine type, and transmission ratio selection). EVs' internal powertrain control variables play an essential role in determining the powertrain efficiency and the resulting EV acceleration. There is scope for incorporating powertrain into the EV running dynamics to derive the optimal eco-driving strategy [4-6]. Most of the previous eco-driving strategies were applied to a specific driving cycle that provides the speed profiles. This means that the above eco-driving strategies ignored the impact of different adopted acceleration on the vehicle performance under different driving scenarios. Simultaneously, the above eco-driving strategies did roughly calculate the SOC since they did not consider each part's efficiency of the powertrain and the battery thermal effect. This motivates us to explore

---

1 the EV eco-driving strategy with the explicit consideration of the different adopted  
2  
3 acceleration, the complete efficiency of the powertrain, and the battery thermal effect.  
4

5  
6 With the rapid development of EVs, researchers have made more and more  
7  
8 researches on the EV powertrain and the EV eco-driving strategy to improve the EVs'  
9  
10 economy and power [7,8]. Although different EV topologies and corresponding  
11  
12 strategies have been proposed, the main powertrain components and their functions are  
13  
14 the same [9,10]. This shows that it is feasible to study the energy consumption of EVs  
15  
16 with a general topological structure. Usually, EV powertrain is composed of battery,  
17  
18 electromotor, transmission, and other transmission devices. As one common energy  
19  
20 storage unit of EVs, the battery performance directly affects EVs' energy consumption  
21  
22 and power performance [11,12]. The lithium-ion battery, now widely used in EVs, is  
23  
24 considered as one of the most promising battery types [13]. The battery models used in  
25  
26 the EV simulation mainly include the equivalent circuit model, the neural network  
27  
28 model, and the simplified electrochemical model [14]. Widanage et al. [15] modeled  
29  
30 and analyzed several kinds of batteries (e.g., lithium battery) using many equivalent  
31  
32 circuit models (e.g., Rint model, RC model, and PNGV model) and pointed out that the  
33  
34 battery equivalent circuit model could be applied to the modeling and analysis of  
35  
36 various kinds of batteries. Wei et al. [16] estimated the SOC and capacity with an online  
37  
38 identified battery model. Li et al. [17] obtained the SOC for a single LiCoO<sub>2</sub> battery  
39  
40 based on the simplified electrochemical model. Therefore, the accurate calculation of  
41  
42 SOC should adequately consider not only the battery performance, but also the thermal  
43  
44 effect and the variable powertrain efficiency.  
45  
46  
47  
48  
49  
50  
51  
52  
53  
54  
55  
56  
57  
58  
59  
60  
61  
62  
63  
64  
65

---

1 Another essential component of the powertrain is the electromotor. According to  
2  
3 the electromagnetic induction law, the electromotor realizes the conversion of electric  
4  
5 energy to mechanical energy, where the primary function is to generate the driving  
6  
7 torque [18,19]. Ming et al. [20] proposed a computationally intelligent methodology  
8  
9 and a sliding mode control for EV, where the quick responsibility and the precision  
10  
11 requirements of the electromotor torque controls were both satisfied. Ji et al. [21]  
12  
13 constructed the concept of "the exertion degree of energy efficiency of electromotor"  
14  
15 to quantitatively evaluate the EV's electromotor efficiency under one specific condition.  
16  
17 Rahman et al. [22] defined the efficiency characteristic of the electromotor as the ratio  
18  
19 of the output power to the input power and found that the electromotor has an optimal  
20  
21 efficiency region. Thus, the performance of electromotor in different working states can  
22  
23 be explored through the relationship among electromotor efficiency, electromotor speed,  
24  
25 and electromotor torque.  
26  
27

28  
29 The powertrain transmission is used to change the speed and torque of the rotating  
30  
31 mechanical energy transferred from the electromotor [23-25]. The development of the  
32  
33 EV powertrain tends to be multi-speed using different transmissions. The multi-speed  
34  
35 transmission can control the powertrain transmission ratio to improve EVs' power  
36  
37 performance and the energy economy. Ruan et al. [26] compared the energy  
38  
39 consumption and the costs of battery based on the different powertrains: a fixed ratio  
40  
41 single reduction powertrain, two-speed powertrain, and one continuously variable  
42  
43 transmission (CVT) powertrain, and showed that the CVT scenario could improve the  
44  
45 overall powertrain efficiency, save battery energy, and reduce customer costs. Hu et al.  
46  
47  
48  
49  
50  
51  
52  
53  
54  
55  
56  
57  
58  
59  
60  
61  
62  
63  
64  
65

---

1 [27] proposed one CVT control strategy to reduce energy loss, enhance energy economy,  
2  
3 and improve driving comfort. As for the other transmission devices in the EV  
4  
5 powertrain, researchers usually take the efficiency as a fixed value [28-30], and the  
6  
7 other transmission devices include the drive shafts, the differential, the final reduction  
8  
9 drive, and the wheels. So, the adjustment effect of CVT can be accurately studied by  
10  
11 analyzing the relationship between the efficiency of CVT and the CVT control variables,  
12  
13 i.e., CVT speed ratio and electromotor torque.  
14  
15  
16  
17  
18  
19

20 A better understanding of the powertrain functions and characteristics is essential  
21  
22 to design an eco-driving strategy that controls EV's running dynamics and minimizes  
23  
24 energy consumption. Through the improvement of driving behavior and regional traffic  
25  
26 flow, eco-driving strategies can lead to the advancement of the local environmental  
27  
28 quality and reduce energy consumption [31]. Okada et al. [32] proposed systems to  
29  
30 anticipate the conditions in front of the vehicle and to control the powertrain by using  
31  
32 external sensing technology. Kato et al. [33] showed that the eco-driving strategy with  
33  
34 the observing limited constant speed was sufficient to reduce the kinematic running  
35  
36 energy. Koch et al. [34] proposed an online nonlinear algorithm to optimize speed  
37  
38 profile and powertrain operation for EVs with multiple motors and multiple gears.  
39  
40 Sayed et al. [35] developed an effective energy management strategy for EV  
41  
42 applications under different driving cycles. Zheng et al. [36] studied the dynamics of  
43  
44 vehicle motion and battery for an integrated EV eco-driving model and showed that the  
45  
46 eco-driving could achieve minimal energy consumption in the driving cycles. Chen et  
47  
48 al. [37] optimized over driving modes of trucks to achieve a trade-off between fuel  
49  
50  
51  
52  
53  
54  
55  
56  
57  
58  
59  
60  
61  
62  
63  
64  
65

---

1 consumption and trip time. Wang et al. [38] conducted a questionnaire survey on EV  
2  
3 drivers' driving behavior and hypothetical decisions of their driving and revealed that  
4  
5 compared to internal combustion engine vehicle drivers, the EV drivers possessed  
6  
7 significantly calmer driving maneuvers and more fuel-efficient driving habits, and were  
8  
9 more willing to use eco-friendly new technologies. Therefore, the eco-driving strategy  
10  
11 based on the powertrain can ensure the EV has the desired performance under realistic  
12  
13 driving conditions by optimizing powertrain control variables.  
14  
15  
16  
17  
18  
19

20 Most of the existing studies so far have focused on the EV powertrain components  
21  
22 and the eco-driving strategy separately. Not only can eco-driving strategy advise on  
23  
24 drivers' driving behavior, with the advancement in automated driving technology, but  
25  
26 there is also potential to achieve eco-driving through the control of the powertrain to  
27  
28 directly replace driving. To our best knowledge, there has been no effort made to study  
29  
30 the eco-driving strategy for EV that explicitly considers both the whole powertrain  
31  
32 functioning and the battery thermal effect for different driving modes (e.g., acceleration  
33  
34 mode (AM), deceleration mode (DM), and uniform motion mode (UMM)). This paper  
35  
36 proposes a holistic solution to obtain the optimal powertrain output variable (including  
37  
38 the battery current, the CVT ratio, and the braking force) for maximal SOC under  
39  
40 different driving modes, where the output the variables that enable the whole powertrain  
41  
42 to cooperate normally are selected from all feasible values by the DP algorithm.  
43  
44 Comparing with the existing studies, this paper has three prominent contributions, i.e.,  
45  
46 (i) the SOC calculation accuracy can be enhanced by considering the complete  
47  
48 powertrain efficiency and battery thermal effect; (ii) optimizing the acceleration of  
49  
50  
51  
52  
53  
54  
55  
56  
57  
58  
59  
60  
61  
62  
63  
64  
65

---

1 different driving modes can make full use of the powertrain coupling effect; and (iii)  
2  
3 The sensitivity of the powertrain to SOC and environment temperature, as well as the  
4  
5 strategy adaptability in urban and suburban driving conditions, are explored.  
6  
7

8  
9 After the introduction, the remainder of this paper is organized as follows: Section  
10  
11 2 analyzes the EV longitudinal dynamics and then proposes the EV dynamics model  
12  
13 that consists of three sub-models, i.e., the battery model considering thermal effect, the  
14  
15 CVT efficiency model, and the electromotor efficiency model. Section 3 describes an  
16  
17 eco-driving strategy for the EV to maximize the SOC under different driving modes  
18  
19 and presents a DP-based solution algorithm, while Section 4 conducts simulation and  
20  
21 discussion to evaluate the proposed strategy feasibility and adaptability. Finally, the  
22  
23 main conclusion and future research directions are presented in Section 5.  
24  
25  
26  
27  
28  
29

## 30 **2. An EV longitudinal dynamics model based on the powertrain**

31  
32

33  
34 An EV powertrain is composed of a battery, electromotor, CVT, and other  
35  
36 transmission devices (Fig. 1) [39]. The driving modes of the EV can be mainly divided  
37  
38 into AM, DM, and UMM, according to the flow direction of power in the powertrain  
39  
40 [40]. During the AM and UMM, the power flow direction is positive, and the braking  
41  
42 force is zero. The battery is used as the energy supply device to transfer the stored  
43  
44 electric energy to the electromotor. After the electric energy is converted into the  
45  
46 electromotor's rotating mechanical energy, it is handled by the CVT. The CVT changes  
47  
48 the speed and the torque of the rotating mechanical energy by adjusting its speed ratio  
49  
50 and then transfers it to other transmission devices (e.g., the final reduction drive), which  
51  
52 in turn drives the wheels to achieve the driving of EV. In contrast, the power flow  
53  
54  
55  
56  
57  
58  
59  
60  
61  
62  
63  
64  
65

direction is opposite, and the braking force is not zero during the DM, where the battery is charged by the energy transformed through the electromotor, the CVT, and the other transmission devices in turn.

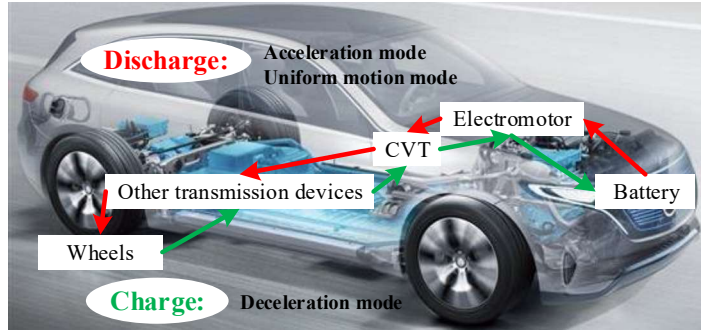


Fig. 1. The main powertrain structure of an EV.

### 2.1. EV longitudinal driving dynamics

In its longitudinal motion, the driving force of the EV needs to balance the driving resistance. According to EV longitudinal dynamics analysis [6], the driving resistance includes rolling resistance, gradient resistance (the component force of the gravity along the direction of the slope), air resistance, acceleration resistance, and braking force (Fig. 2).

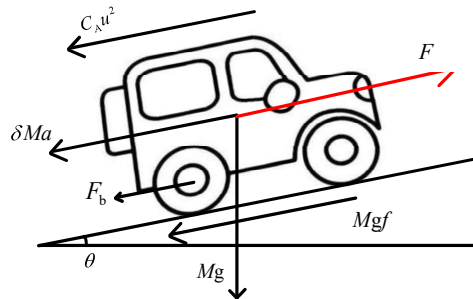


Fig. 2. The forces acting on the EV during driving.

In driving the EV, its powertrain is required to provide the needed driving force to achieve the required accelerations at different EV speeds, and its value is changing over time  $t$ , i.e.,

$$F(t) = Mgf + Mg\theta + C_A u(t)^2 + \delta Ma(t) + F_b(t) \quad (1)$$

where  $t$  is the time instant (s),  $F$  is the needed driving force (N),  $M$  is the EV mass (kg),  $g$  is the acceleration due to gravity ( $\text{m/s}^2$ ),  $f$  is the coefficient of rolling resistance,  $\theta$  is the road slope,  $C_A$  is the aerodynamic drag coefficient ( $\text{kg/m}$ ),  $u$  is the EV speed ( $\text{m/s}$ ),  $\delta$  is the mass factor,  $a$  is the EV acceleration ( $\text{m/s}^2$ ), and  $F_b$  is the braking force (N) which is controlled by the brake and limited by the adhesion between ground and wheels.

During the driving process, the EV speed can be calculated as follows:

$$u(t+\Delta t) = u(t) + \int_t^{t+\Delta t} a(t) dt \quad (2)$$

where  $\Delta t$  is the time gap (s).

## 2.2. Battery model considering thermal effect

The EV battery is made up of a series of lithium battery cells. In this paper, all battery cells have the same working state, in that the change of SOC and battery temperature are the same. To simulate the battery's dynamic voltage characteristics, the equivalent circuit model that uses resistance, capacitance, constant voltage source, and other circuit elements to form a circuit network is adopted here. This kind of model is a lumped parameter model and usually contains relatively few parameters. Thus, it is easy to derive the equivalent circuit model, so it is widely used in system simulation and control [41].

The battery cell characteristic is represented by the Rint model (Fig. 3), where the battery cell is equivalent to a series connection of ideal voltage source and battery internal resistance, and the battery performance varies with battery temperature and SOC [5, 42-44]. To improve the model accuracy, the battery thermal effect is considered to calculate the battery temperature change, taking the battery temperature as a variable value and calculating the heat generated by the battery in the processes of charging and discharging. Thus, this paper introduces the battery thermal effect into the Rint model to present the battery characteristics based on the SOC and battery temperature, which allows the constructed model to calculate the changes of SOC and battery temperature according to the battery current.

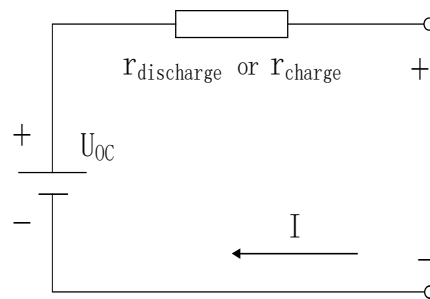


Fig. 3. The battery Rint model.

Next, this paper examines the change of SOC. SOC is the remaining power of the battery, i.e., the ratio of the remaining capacity to the total available capacity after the battery is used or kept for a long time. During AM and UMM, the braking force is zero, i.e., the battery should provide the power to drive the EV. During DM, the braking force is larger than zero, i.e., the battery is charged by the EV. Thus, the SOC can be calculated according to the battery current, i.e.,

$$SOC(t+\Delta t) = \begin{cases} SOC(t) - \frac{\int_t^{t+\Delta t} I(t) dt}{C_{\text{battery}}}, & \text{if } F_b(t) = 0 \\ SOC(t) + \frac{\int_t^{t+\Delta t} I(t) dt}{C_{\text{battery}}}, & \text{if } F_b(t) > 0 \end{cases} \quad (3)$$

where  $SOC$  is the battery state of charge (%),  $C_{\text{battery}}$  is the battery's original full capacity of the battery (Ah), and  $I$  is the battery current (A). For simplicity, this paper assumes that  $C_{\text{battery}}$  is a constant since the changes in capacity are very small in a short time operation.

Through simple circuit analysis and calculation based on the Rint model, the battery power can be expressed as,

$$P_{\text{battery}}(t) = \begin{cases} n_{\text{cell}} \left( U_{\text{OC}}(t) I(t) - I(t)^2 r_{\text{discharge}} \right), & \text{if } F_b(t) = 0 \\ n_{\text{cell}} \left( U_{\text{OC}}(t) I(t) + I(t)^2 r_{\text{charge}} \right), & \text{if } F_b(t) > 0 \end{cases} \quad (4)$$

where  $P_{\text{battery}}$  is the battery power (kW),  $n_{\text{cell}}$  is the number of battery cells,  $U_{\text{OC}}$  is the open circuit voltage of the battery cell (V), and  $r_{\text{discharge}}$  and  $r_{\text{charge}}$  is the discharge and charge resistance of the battery cell ( $\Omega$ ), respectively.

As the energy store device of EV, the battery needs to provide enough power to ensure the normal driving of EV, so the battery should adjust the battery current to produce the required battery power according to the EV kinetic equation, i.e.,

$$P_{\text{battery}}(t) = \begin{cases} F(t) u(t) \eta_{\text{battery}}(t) / \eta_{\text{EV}}(t), & \text{if } F_b(t) = 0 \\ F_b(t) u(t) \eta_{\text{EV}}(t) / \eta_{\text{battery}}(t), & \text{if } F_b(t) > 0 \end{cases} \quad (5)$$

where  $\eta_{\text{EV}}$  is the EV efficiency (%), and can be defined as follows:

$$\eta_{\text{EV}}(t) = \eta_t \eta_{\text{cvt}}(t) \eta_{\text{em}}(t) \eta_{\text{battery}}(t) \quad (6)$$

where  $\eta_t$  is the powertrain efficiency without CVT and electromotor (%),  $\eta_{cvt}$  is the CVT efficiency (%),  $\eta_{em}$  is the electromotor efficiency (%), and  $\eta_{battery}$  is the battery efficiency (%), and can be calculated as,

$$\eta_{battery}(t) = \begin{cases} \frac{U_{OC}(t)I(t) - I(t)^2 r_{discharge}(t)}{U_{OC}(t)I(t)}, & \text{if } F_b(t) = 0 \\ \frac{U_{OC}(t)I(t)}{U_{OC}(t)I(t) + I(t)^2 r_{charge}(t)}, & \text{if } F_b(t) > 0 \end{cases} \quad (7)$$

It is noted that  $U_{OC}$ ,  $r_{discharge}$  and  $r_{charge}$  are all varying with the SOC and the battery temperature according to the battery thermal effect [5,42-44]. And, the corresponding numerical relationships can be defined by Eqs. (8-10) through the polynomial functions:

$$U_{OC}(T(t), SOC(t)) = \sum_{n=0}^{N_{OC}^1} \sum_{m=0}^{N_{OC}^2-n} A_{nm}^{OC} T(t)^n SOC(t)^m \quad (8)$$

$$r_{discharge}(T(t), SOC(t)) = \sum_{n=0}^{N_{discharge}^1} \sum_{m=0}^{N_{discharge}^2-n} A_{nm}^{discharge} T(t)^n SOC(t)^m \quad (9)$$

$$r_{charge}(T(t), SOC(t)) = \sum_{n=0}^{N_{charge}^1} \sum_{m=0}^{N_{charge}^2-n} A_{nm}^{charge} T(t)^n SOC(t)^m \quad (10)$$

where  $A_{nm}^{OC}$ ,  $N_{OC}^1$ ,  $N_{OC}^2$ ,  $A_{nm}^{discharge}$ ,  $N_{discharge}^1$ ,  $N_{discharge}^2$ ,  $A_{nm}^{charge}$ ,  $N_{charge}^1$ ,  $N_{charge}^2$  denote the regression coefficient, 1<sup>st</sup> variable degree and 2<sup>nd</sup> variable degree of the polynomial fitting function of  $U_{OC}$ ,  $r_{discharge}$  and  $r_{charge}$ , respectively. And all of them can be calibrated by the data collected from the battery load characteristics experiments.

It is noted that the utilized data [42] is presented along with the corresponding map of the fitting functions in Fig. 4. And, the relevant values of the fitting functions are shown in Tables 1-3 (Appendix). It can be seen from Fig. 4 that battery performance is closely related to environment temperature and SOC. With the decrease of SOC, the sensitivity of open circuit voltage to temperature increases. There will be a big

1 difference between the charging process and the discharging process due to the apparent  
 2  
 3 difference in battery internal resistance.  
 4  
 5

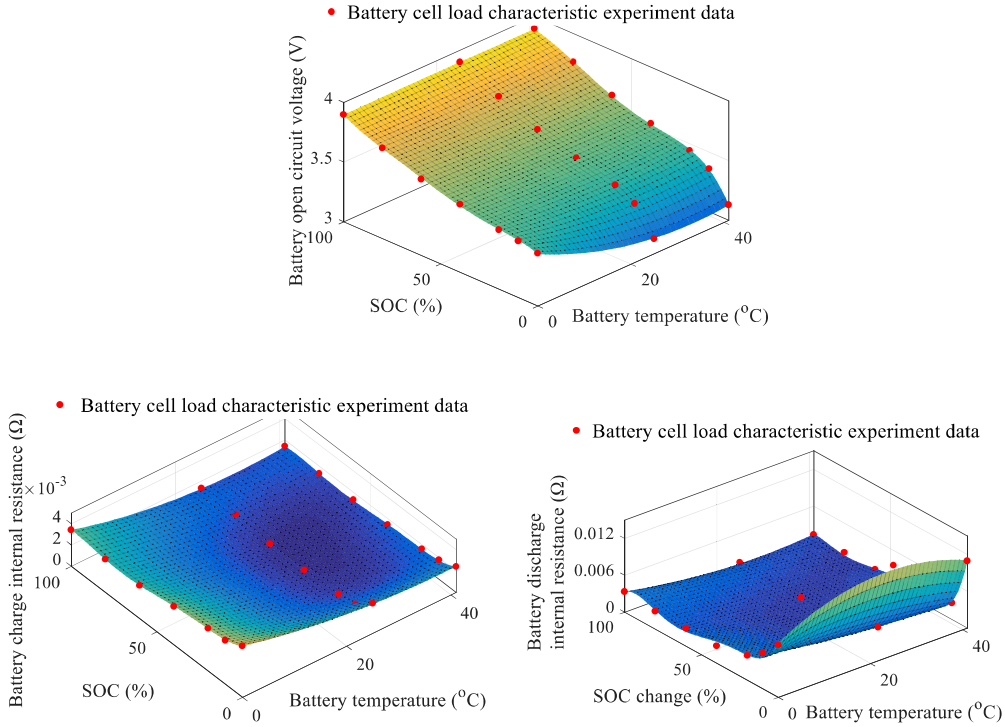


Fig. 4. Open circuit voltages, discharge resistance, and charge resistance of the battery cell and the data collected from the battery cell load characteristic experiment.

Then, this paper calculates the change of battery temperature. According to the battery thermal effect, the battery temperature change can be formulated as follows:

$$T(t+\Delta t) = T(t) + \int_t^{t+\Delta t} \frac{n_{\text{cell}} (Q_{\text{battery}}(t) - Q_a(t))}{m_{\text{battery}} c_{\text{battery}}} dt \quad (11)$$

where  $T$  is the battery working temperature ( $^{\circ}\text{C}$ ),  $Q_{\text{battery}}$  is the heat generated by the battery cell (J),  $Q_a$  is the heat emitted into the air of the battery cell (J),  $m_{\text{battery}}$  is the battery mass (kg), and  $c_{\text{battery}}$  is the battery components specific heat ( $\text{Jkg}^{-1}\text{K}^{-1}$ ).

Here, the heat source inside the battery cell is stable and uniform. According to the typical model of battery heat generation established by Bemadi [45], the heat generated by the battery cell can be formulated as follows:

$$Q_{\text{battery}}(t) = \begin{cases} I(t)^2 r_{\text{discharge}}(t) - I(t)T(t) \frac{dU_{\text{oc}}(t)}{dT(t)}, & \text{if } F_b = 0 \\ I(t)^2 r_{\text{charge}}(t) - I(t)T(t) \frac{dU_{\text{oc}}(t)}{dT(t)}, & \text{if } F_b > 0 \end{cases} \quad (12)$$

where  $I^2 r_{\text{discharge}}$  and  $I^2 r_{\text{charge}}$  are respectively the sum of battery cell Joule heat and polarization heat in discharge and charge state, and  $IT \frac{dU_{\text{oc}}}{dT}$  is the heat of electrochemical reaction.

The heat emitted into the air of the battery cell can be formulated as follows [46]:

$$Q_a(t) = \alpha S_{\text{battery}} (T(t) - T_{\text{environment}}) \quad (13)$$

where  $\alpha$  is the heat exchange coefficient of the battery cell ( $\text{W}/(\text{m}^2\text{K})$ ),  $S_{\text{battery}}$  is the surface area of the battery cell ( $\text{m}^2$ ), and  $T_{\text{environment}}$  is the environment temperature ( $^{\circ}\text{C}$ ).

### 2.3. Electromotor efficiency model

The electromotor's primary function is to convert the electric energy generated from the battery into rotating mechanical energy through the medium of the magnetic field, and then transfer the energy to CVT. The electromotor characteristics are mainly manifested by electromotor speed, electromotor torque, and electromotor efficiency [18-22]. Thus, the electromotor efficiency model can be described as a function of electromotor speed and electromotor torque to obtain the numerical relationship among electromotor efficiency, electromotor speed, and electromotor torque, i.e.,

$$\eta_{em}(n_{em}(t), T_{em}(t)) = \sum_{n=0}^{N_{em}^1} \sum_{m=0}^{N_{em}^2-n} A_{nm}^{em} n_{em}(t)^n T_{em}(t)^m \quad (14)$$

where  $n_{em}$  is the electromotor speed (r/min),  $T_{em}$  is the electromotor torque (Nm),  $N_{em}^1$  is the 1<sup>st</sup> variable degree of the polynomial fitting function of  $\eta_{em}$ ,  $N_{em}^2$  is the 2<sup>nd</sup> variable degree of the polynomial fitting function of  $\eta_{em}$ , and  $A_{nm}^{em}$  is the corresponding regression coefficient. It is noted that  $N_{em}^1, N_{em}^2$  and  $A_{nm}^{em}$  can be calibrated by fitting the data of the electromotor load characteristic experiment, and the detailed data [42] is presented along with the map of the fitting functions in Fig.5. And the relevant values of the fitting functions are shown in Table 4 (Appendix). From Fig. 5, the electromotor has a high-efficiency working area, where efficiency will be significantly reduced once the electromotor torque and speed exceeds the area.

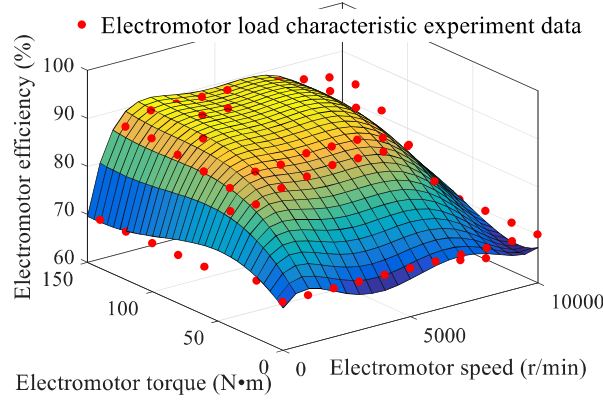


Fig. 5. Electromotor efficiency and the data collected from the electromotor load characteristic experiment.

Here,  $n_{em}(t)$  and  $T_{em}(t)$  are formulated based on the vehicle powertrain as follows:

$$n_{em}(t) = \frac{30i_o i_{cvt}(t)u(t)}{\pi r} \quad (15)$$

$$T_{em}(t) = \begin{cases} \frac{9550n_{cell} (U_{OC}(t)I(t) - I(t)^2 r_{discharge})}{n_{em}(t)}, & \text{if } F_b(t) = 0 \\ \frac{9550n_{cell} (U_{OC}(t)I(t) + I(t)^2 r_{charge})}{n_{em}(t)}, & \text{if } F_b(t) > 0 \end{cases} \quad (16)$$

where  $i_o$  is the final reduction drive speed ratio,  $i_{cvt}$  is the CVT speed ratio,  $r$  is the wheel radius (m).

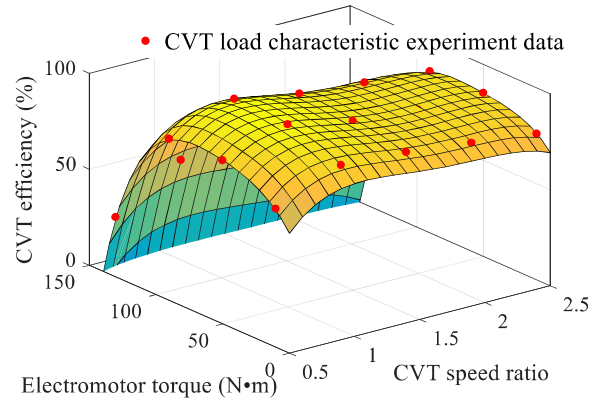
#### 2.4. CVT efficiency model

The CVT is used to change the speed and the torque of the rotating mechanical energy transferred from the electromotor, and then drive the wheels with the help of other transmission devices. As part of the EV powertrain, the CVT can realize the optimal operation of the EV powertrain through continually adjusting the CVT speed ratio to achieve the coordinating working states of the battery, the CVT, and the electromotor in AM and UMM, and CVT can also improve the efficiency of the regenerative braking energy recovery in DM [23-25]. Thus, like the electromotor efficiency model, the CVT efficiency model can be defined as a function of the CVT speed ratio and the electromotor torque, i.e.,

$$\eta_{cvt}(i_{cvt}(t), T_{em}(t)) = \sum_{n=0}^{N_{cvt}^1} \sum_{m=0}^{N_{cvt}^2 - n} A_{nm}^{cvt} i_{cvt}(t)^n T_{em}(t)^m \quad (17)$$

where  $N_{cvt}^1$  is the 1<sup>st</sup> variable degree of the polynomial fitting function of  $\eta_{cvt}$ ,  $N_{cvt}^2$  is the 2<sup>nd</sup> variable degree of the polynomial fitting function of  $\eta_{cvt}$ , and  $A_{nm}^{cvt}$  is the corresponding regression coefficient. And, all of them can be obtained based on the data collected from the CVT load characteristic experiment. It is noted that the detailed data [23-25] is presented with the map of the function in Fig. 6. Like the electromotor, the relevant values of the fitting functions are shown in Table 5 (Appendix). Based on

1 Fig. 6, the CVT also has a high-efficiency working area, where efficiency will be  
2 significantly reduced once the electromotor torque exceeds the area.  
3  
4



21 Fig. 6. CVT efficiency and the data collected from the CVT load characteristic  
22 experiment.  
23  
24  
25  
26

### 27 3. Eco-driving strategy for basic driving modes

28  
29 The EV driving can be broadly considered to compose of three basic modes  
30 according to the power flow in the powertrain: (i) AM, (ii) DM, (iii) UMM. The eco-  
31 driving strategy is then proposed for each of the three driving modes. Besides, the  
32 strategy input variable needs to reflect the specific driving requirements in different  
33 driving modes, and the strategy output variable should control the powertrain to satisfy  
34 the corresponding driving requirements.  
35  
36  
37  
38  
39  
40  
41  
42  
43  
44  
45

46 As far as the input variable of the driving strategy is concerned, the strategies  
47 applicable to different driving modes should meet the corresponding driving  
48 requirements according to the input variable. When the EV speed needs to be changed,  
49 the driving requirement at this time is the EV speed-change. When the desired EV speed  
50 is greater than the current EV speed, AM is adopted, but in the opposite situation, DM  
51 is adopted. In addition, once the EV speed has reached the desired EV speed, the driving  
52  
53  
54  
55  
56  
57  
58  
59  
60  
61  
62  
63  
64  
65

---

1 requirement is to drive a certain distance in UMM. Therefore, the speed-change is the  
2 input variable of AM and DM, and the input variable of UM is driving distance. As for  
3 the powertrain control variables, the battery current and the CVT speed ratio are  
4 adopted as the control variables in AM and DM, as the powertrain power flow is in a  
5 positive direction. On the contrary, the power flows is in the reverse direction in DM,  
6 so the control variables contain the braking force and the CVT speed ratio. Thus, the  
7 eco-driving strategy is formulated as a global optimization problem, where the decision  
8 variables are the powertrain control variables, which include the battery current, the  
9 CVT speed ratio, and the braking force. The optimization's objective is to maximize  
10 *SOC* for each of the driving modes. According to the EV dynamics model described  
11 in Section 2 and the above analysis, the optimal powertrain control variables can be  
12 calculated from the EV's driving requirements. This paper defines a general input  
13 variable  $X(t)$  and an output variable  $Y(t)$  as follows:

$$34 \quad X(t) = \begin{cases} [u_{\text{start}}(t), u_{\text{end}}(t)], & \text{if EV is in AM or DM} \\ s(t), & \text{if EV is in UMM} \end{cases} \quad (18)$$

35 where  $u_{\text{start}}$  is the start EV speed (m/s),  $u_{\text{end}}$  is the end EV speed (m/s), and  $s(t)$   
36 is the expected driving distance.

$$37 \quad Y(t) = [I(t), i_{\text{cvt}}(t), F_b(t)] \quad (19)$$

38 The objective is to derive the appropriate output variable that optimizes *SOC* for  
39 the different driving modes while ensuring the operational limit of the powertrain and  
40 the driving comfort. Therefore, the eco-driving strategy is a nonlinear optimization  
41 problem with constraints. During the process when the EV accomplishes the driving  
42

requirements from time  $t$  to time  $t_{\text{end}}$ , the objective function can be designed as follows:

$$\max SOC(t_{\text{end}}) \quad (20)$$

where  $t_{\text{end}}$  is the time when the driving requirement is accomplished.

In order to ensure the operational safety of powertrain and the driving comfort, we use the lower and upper bounds to guarantee the working of the EV [5-8], and the constraints of the optimization problem are as follows:

(1) The EV speed constraint:

$$u_{\min} \leq u \leq u_{\max} \quad (21a)$$

(2) The EV comfortable constraint:

$$a_{\min} \leq a \leq a_{\max} \quad (21b)$$

(3) The CVT safety constraint:

$$i_{\text{cvtmin}} \leq i_{\text{cvt}} \leq i_{\text{cvtmax}} \quad (21c)$$

(4) The electromotor safety constraint:

$$T_{\text{emmin}} \leq T_{\text{em}} \leq T_{\text{emmax}} \quad (21d)$$

(5) The brake force constraint:

$$0 \leq F_b \leq Mg\mu \quad (21e)$$

where  $\mu$  is the coefficient of sliding resistance.

(6) The battery safety constraint:

$$I_{\min} \leq I \leq I_{\max} \quad (21f)$$

---

Here,  $u_{\min}$ ,  $u_{\max}$ ,  $a_{\min}$ ,  $a_{\max}$ ,  $i_{\text{cvtmin}}$ ,  $i_{\text{cvtmax}}$ ,  $T_{\text{emmin}}$ ,  $T_{\text{emmax}}$ ,  $I_{\min}$ ,  $I_{\max}$  denote the lower and upper bounds of the EV speed, acceleration, CVT speed ratio, electromotor torque, and battery current, respectively.

Based on the Behrman optimization that uses the multi-stage decision to obtain the optimal strategy [47-49], we design a DP algorithm to solve the optimization problem, where the algorithm can be formulated as follows:

---

The DP algorithm of the eco-driving strategy for EV based on the powertrain

---

### Step 1: Initialization

At the time  $t$ , input  $X(t)$  according to the driving requirement, and obtain the powertrain working state variables required for calculation ( $u(t)$ ,  $T(t)$  and  $SOC(t)$ )

It is noted that  $u_{\text{start}}(t)$  is  $u(t)$  during the driving modes, i.e.,

$$u_{\text{start}}(t) = u(t)$$

### Step 2: Determine the driving scenario

If  $X(t) = [u_{\text{start}}(t), u_{\text{end}}(t)]$  and  $u_{\text{start}}(t) < u_{\text{end}}(t)$ ,  $F_b(t) = 0$ , the driving mode is acceleration

If  $X(t) = [u_{\text{start}}(t), u_{\text{end}}(t)]$  and  $u_{\text{start}}(t) > u_{\text{end}}(t)$ ,  $0 < F_b(t) \leq Mg\mu$ , the driving mode is deceleration

If  $X = s(t)$ ,  $F_b(t) = 0$ , the driving mode is uniform motion

### Step 3: Discretization

Discretize  $X(t)$  and all possible  $Y(t)$  to calculate all available driving modes with the constraints

(i) AM or DM

Discrete  $u$  into  $N$  values between  $u_{\text{start}}(t)$  and  $u_{\text{end}}(t)$

Discrete  $I$  and  $i_{\text{cvt}}$  into  $m$  and  $k$  values respectively in acceleration scenario according to the constraints. It is noted that in this scenario  $F_b(t) = 0$ .

Likely, Discrete  $i_{\text{cvt}}$  and  $F_b$  into  $k$  and  $x$  values respectively in the deceleration scenario. It is noted that  $I$  can be calculated from Eqs. (5) and (6) in the deceleration scenarios, i.e.,

$$I(t) = \frac{U_{\text{OC}}(t) - \sqrt{U_{\text{OC}}(t)^2 + 4r_{\text{charge}}(t)F_b(t)u(t)\eta_{\text{EV}}(t)/(n_{\text{cell}}\eta_{\text{battery}}(t))}}{2r_{\text{charge}}(t)}$$

And according to Eqs. (5), (7), (9), and (14-17),  $I(t)$  can be calculated by  $u(t), T(t), SOC(t), i_{\text{cvt}}(t)$  and  $F_b(t)$

#### (ii) UMM

Discrete  $s$  into  $Z$  values

Discrete  $I$  and  $i_{\text{cvt}}$  into  $m$  and  $k$  values respectively according to the constraints, and  $F_b(t) = 0$

#### Step 4: Choose the optimal output at ith stage

If the driving scenario is acceleration or deceleration: take  $u$  as the stage variable. Otherwise, we take  $S$  as the stage variable. Thus, the objective function can be obtained:

$$\max L_Y(I, i_{\text{cvt}}, F_b, N) + \sum_{i=0}^{Y-1} L_i(I, i_{\text{cvt}}, F_b, i)$$

where  $L_i$  is the stage value from the  $i$ th stage to the  $(i+1)$ th stage,  $L_Y$  is the terminal value. In this paper, we set  $L_Y$  as 0

At the  $i$ th stage,  $L_i$  can be formulated simply according to Eq. (3), i.e.,

$$L_i = \begin{cases} SOC(t_i) - \frac{I\Delta t_i}{C_{\text{battery}}}, & \text{if } F_b = 0 \\ SOC(t_i) + \frac{I\Delta t_i}{C_{\text{battery}}}, & \text{if } F_b > 0 \end{cases}$$

where  $t_i$  is the time of the  $i$ th stage,  $\Delta t_i$  is the time gap at the  $i$ th stage, and can be formulated as follows:

$$t_i = t + \sum_{j=1}^i \Delta t_j$$

Here, the value of acceleration is thought to be constant at the  $i$ th stage, i.e.,

$$\Delta t_i = \begin{cases} \left| \frac{u(t_i) - u(t_{i+1})}{a(t_i)} \right|, & \text{if EV is in AM or DM} \\ \frac{s(t_i)}{u(t_i)(Z+1)}, & \text{if EV is in UMM} \end{cases}$$

where  $a(t_i)$  can be calculated by the Eq. (1), (4), and (5), i.e.,

when  $F_b = 0$

$$a(t_i) = \frac{(U_{oc}(t_i)I(t_i) - I(t_i)^2 r_{\text{discharge}}(t_i))\eta_{em}(t_i)\eta_{cvt}(t_i)}{u(t_i)} - Mgf - Mg\theta - C_A u(t_i)^2$$

And according to Eq. (8), (9), and (14-17),  $a(t_i)$  can be calculated by  $u(t_i), T(t_i), SOC(t_i), I(t_i)$  and  $i_{cvt}(t_i)$

when  $F_b > 0$

$$a(t_i) = -\frac{F_b(t_i) + Mgf + Mg\theta + C_A u(t_i)^2}{\delta M}$$

So, after introducing the discrete values into the calculation, all of the possible driving modes can be obtained, and the optimal  $Y(t_i)$  can be chosen to achieve the maximum  $L_i$  in the eco-driving strategy

**Step 5: Update  $u, T$  and  $SOC$  at  $i+1$ th stage**

---

---

1 Update  $u(t_{i+1}), SOC(t_{i+1})$  and  $T(t_{i+1})$  based on the obtained  $Y(t_i)$

2  
3 According to Eqs. (2), (3), and (11-13), the optimal  $Y(t_i)$  can update  
4  
5  
6  $u(t_{i+1}), SOC(t_{i+1})$  and  $T(t_{i+1})$   
7  
8

#### 9 **Step 6: Obtain the optimal eco-driving strategy**

10  
11 Utilize the basic principle of DP at each stage, the optimal output variable used in the  
12  
13 eco-driving strategy can be calculated after the specific driving requirements ( $u_{start}(t)$   
14  
15 and  $u_{end}(t)$  in the process of acceleration or deceleration, and the driving distance  
16  
17  $s(t)$  in the process of uniform motion) are known  
18  
19  
20  
21

---

22  
23 Thus, the proposed DP algorithm can calculate the eco-driving strategy in different  
24  
25 modes once the specific driving requirements are known. As for the algorithm, we  
26  
27 should give the following note: the error occurs during the discretization but will drop  
28  
29 when the discrete degrees increase, i.e., the numerical solution is closer to the optimal  
30  
31 solution, but the calculation amount rapidly increases.  
32  
33  
34  
35

### 36 **4. Simulation and discussion**

37  
38 This section details the proposed eco-driving strategy's performance for three basic  
39  
40 driving modes under different SOC and environment temperature. To test the  
41  
42 application of the proposed strategy in urban and suburban driving conditions, the  
43  
44 results achieved with the implementation of the strategy under the realistic driving  
45  
46 condition based on the NEDC are presented here. And, then some reflections, involved  
47  
48 with EV energy performance, powertrain optimization potential, and EV optimization  
49  
50 guidelines, are conducted based on the strategy feasibility and adaptability. In addition,  
51  
52  
53  
54  
55  
56  
57  
58  
59  
60  
61  
62  
63  
64  
65

the EV parameters are listed in Table 6 (Appendix), and the simulation parameters are listed in Table 7 (Appendix).

To intuitively display the relationships between the EV running state and the powertrain working state after the proposed strategy is implemented, the speed-change is used to replace the time-change in the simulation.

#### 4.1 Eco-driving strategy feasibility during the AM

During the simulated AM, the EV speed increases from 0m/s to 45m/s which is equal to 162Km/h. In order to explore the performance of the proposed strategy at different SOC's, the environment temperature is 27°C, and the initial SOC is 10%, 20%, 30%, 50%, and 70%, respectively. To explore the proposed strategy's performance at different environment temperatures, the initial SOC is 70%, and the environment temperature is 37°C, 27°C, 17°C, and -17°C. And, the EV's longitudinal dynamics, optimal output variable, and powertrain working state are shown below.

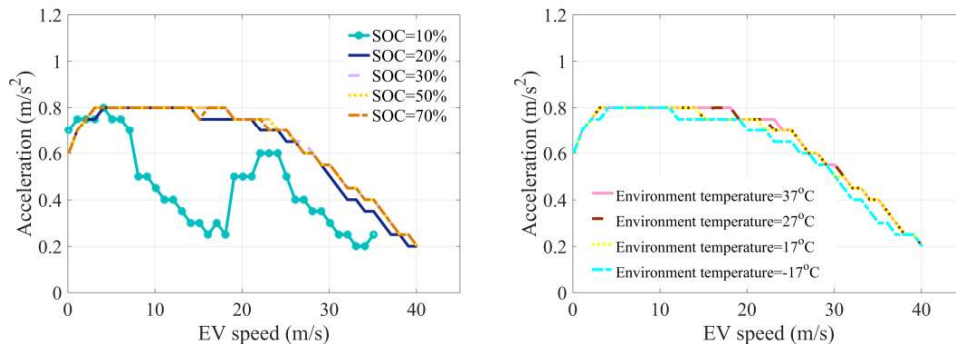
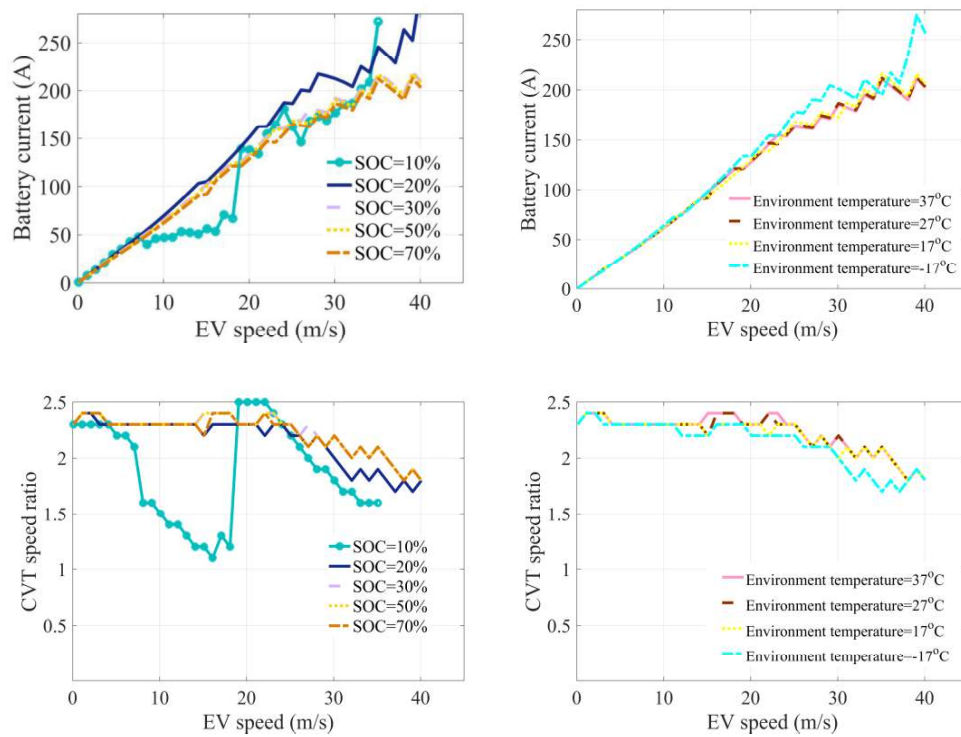


Fig. 7. Acceleration during the AM under different SOC's and environment temperatures.

The first is the EV's longitudinal dynamics, that is, the corresponding acceleration at different EV speeds under different SOC's and environment temperatures, as shown

1 in Fig. 7. The magnitude of acceleration presents a changing trend of "increasing-slowly  
 2 decreasing-sharp decreasing", and the maximum value is  $0.8 \text{ m}^2/\text{s}$ . It is worth noting  
 3 that the extremely low SOC reaching 10% can drastically disturb the powertrain,  
 4 causing an acceleration reduction up to 68.75% in AM when the EV speed is 16.1m/s,  
 5 while the acceleration change, caused by the environment temperature difference, is not  
 6 apparent.



7  
8  
9  
10  
11  
12  
13  
14  
15  
16  
17  
18  
19  
20  
21  
22  
23  
24  
25  
26  
27  
28  
29  
30  
31  
32  
33  
34  
35  
36  
37  
38  
39  
40  
41  
42  
43  
44  
45  
46  
47  
48  
49  
50  
51  
52  
53  
54  
55  
56  
57  
58  
59  
60  
61  
62  
63  
64  
65

Fig. 8. Optimal output variable (battery current and CVT speed ratio) during the AM under different SOC and environment temperatures.

In Fig. 8, the optimal output variable of the strategy is presented, which contains the control variables of the powertrain achieving the eco-driving in the AM. The control of the EV powertrain is embodied in that the battery current can decide the battery output power, and the CVT speed ratio can adjust the powertrain efficiency. As the EV

speed increases to 45m/s, in terms of battery current, the power required by the EV increases, which requires the battery current to continue to increase to 280A. The CVT speed ratio maintains an immense value reaching 2.4, and then drops due to the powertrain declining demand to reduce the rotational speed of the electromotor's rotational energy and increase the torque. So, this phenomenon fully shows the internal coupling effect of the powertrain after adopting the proposed strategy.

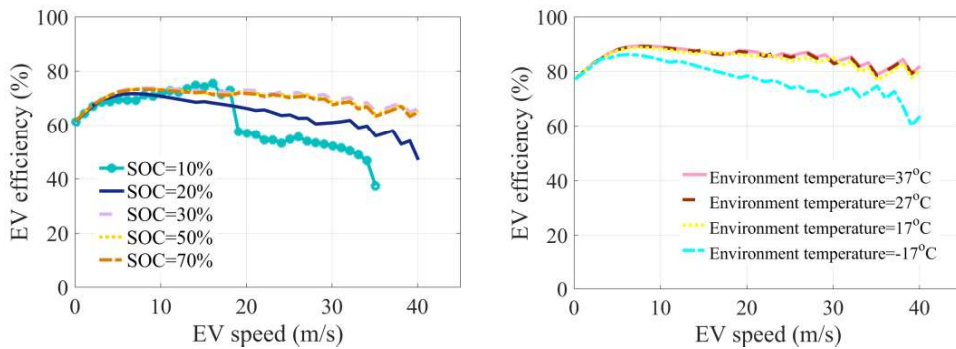


Fig. 9. EV efficiency during the AM under different SOC and environment temperatures.

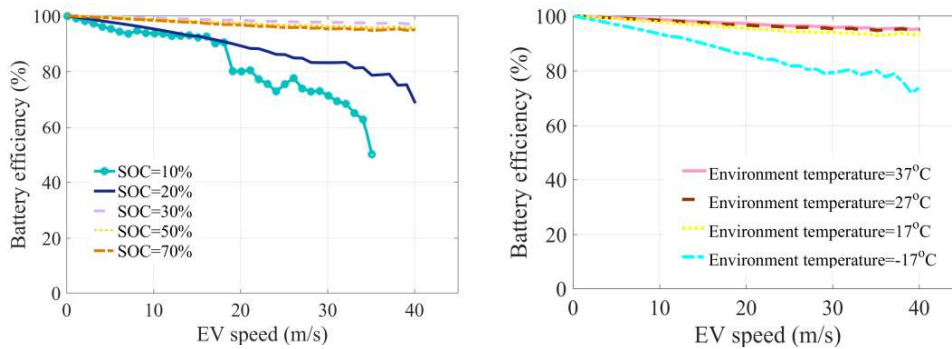


Fig. 10. Battery efficiency during the AM under different SOC and environment temperatures.

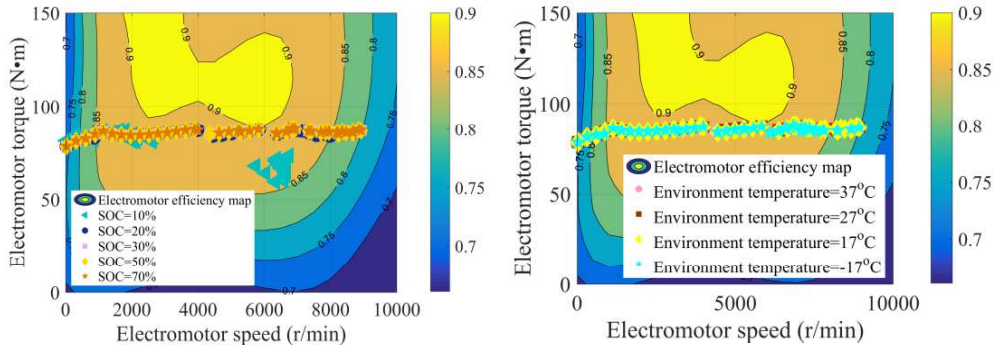


Fig. 11. Electromotor working state during the AM under different SOC and environment temperatures.

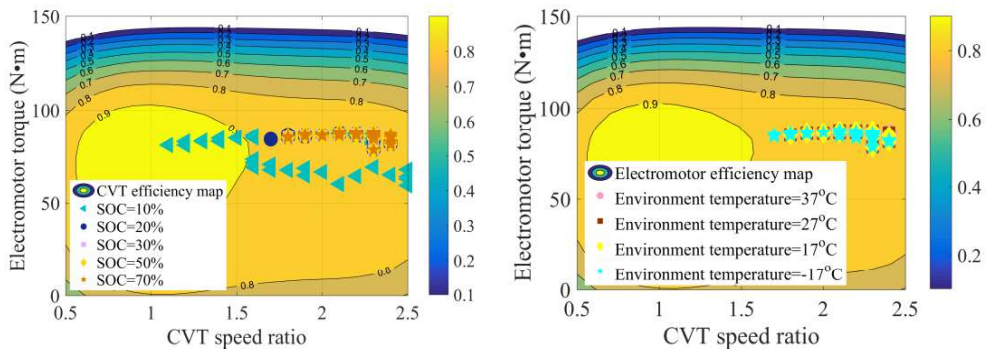


Fig. 12. CVT working state during the AM under different SOC and environment temperatures.

According to the powertrain working state (Figs. 9-12), EV efficiency decreases from 55.88% to 37.37% once the SOC changes from 20% to 10% when the EV speed is 35.1m/s, and the battery efficiency has the same trend. It is noted that low SOC and environment temperature will significantly reduce the battery's efficiency, and low SOC will disturb the entire powertrain, manifesting as a significant change in the speed ratio of CVT, while low environment temperature will not. The above phenomenon can be explained by battery deterioration and powertrain's internal coupling effect very well. The battery performance under low SOC is susceptible to the change of SOC, and the

---

1 specific realization is that the discharge internal resistance increases rapidly and the  
2  
3 open circuit voltage decreases rapidly, thus showing a substantial deterioration of  
4  
5 battery performance under low SOC. On the contrary, the battery performance is  
6  
7 relatively slow to temperature changes, that is, as the temperature decreases, the  
8  
9 discharge internal resistance rises slowly, and the open circuit voltage is nearly  
10  
11 unchanged. Besides, the powertrain's internal coupling effect is mainly determined by  
12  
13 the restriction of the electromotor and the regulating effect of the CVT. The high-  
14  
15 efficiency working area of the electromotor is small, and it is inevitable to run in the  
16  
17 low-efficiency area when the EV speed is low and high, which shows its limitation. In  
18  
19 contrast, the CVT has higher efficiency and a large high-efficiency working area.  
20  
21 Therefore, the CVT can reduce the speed of the rotational energy transmitted by the  
22  
23 electromotor at a larger speed ratio while increasing its torque so as to improve the  
24  
25 power performance of the whole EV.  
26  
27

#### 28 4.2 Eco-driving strategy feasibility during the DM

29 The simulated DM to study the difference caused by the SOC is that the EV speed  
30  
31 decelerates from 45m/s to 0m/s when the environment temperature is 27°C , and the  
32  
33 initial SOC is 10%, 20%, 30%, 50%, and 70%. Besides, to explore the effect of different  
34  
35 environment temperatures on the powertrain, the initial SOC is 70%, and the  
36  
37 environment temperature is 37°C , 27°C , 17°C , and -17°C , respectively. Like the  
38  
39 acceleration process, the acceleration, the powertrain control variables, and the  
40  
41 powertrain working state are shown in Fig. 13-18.  
42  
43  
44  
45  
46  
47  
48  
49  
50  
51  
52  
53  
54  
55  
56  
57  
58  
59  
60  
61  
62  
63  
64  
65

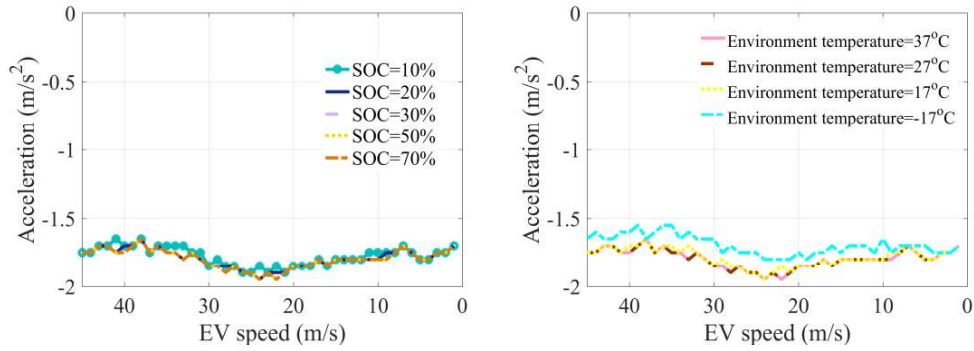
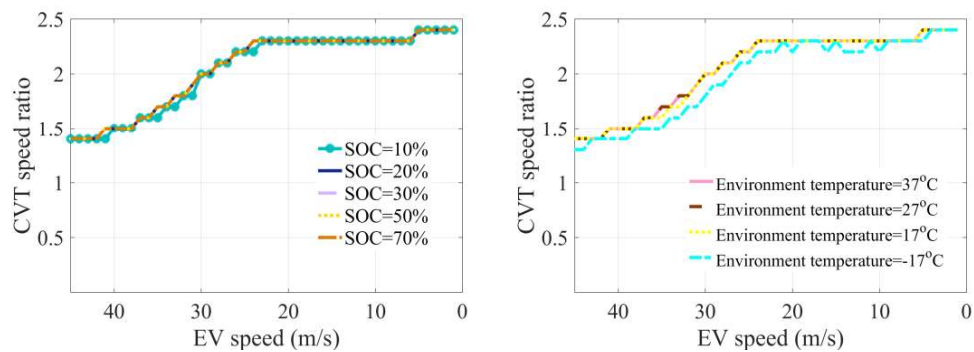


Fig. 13. Acceleration during the DM under different SOC and environment temperatures.

As shown in Fig. 13, the changes in acceleration are relatively gentle and have little relationship with SOC and environment temperature, and the acceleration is fluctuating around  $-1.5 \text{ m}^2/\text{s}$ . However, the overall acceleration will increase to nearly 8.82% at low environment temperatures. The fundamental difference between the acceleration process and the deceleration process stems from the difference in the direction of power flow, and the apparent difference is that the acceleration during the deceleration process remains almost unchanged, which is caused by the braking energy recovery of the EV during the deceleration process. According to Eq. (1), the acceleration is mainly affected by the braking force and wind resistance which is proportional to the third power of the speed during the deceleration process.



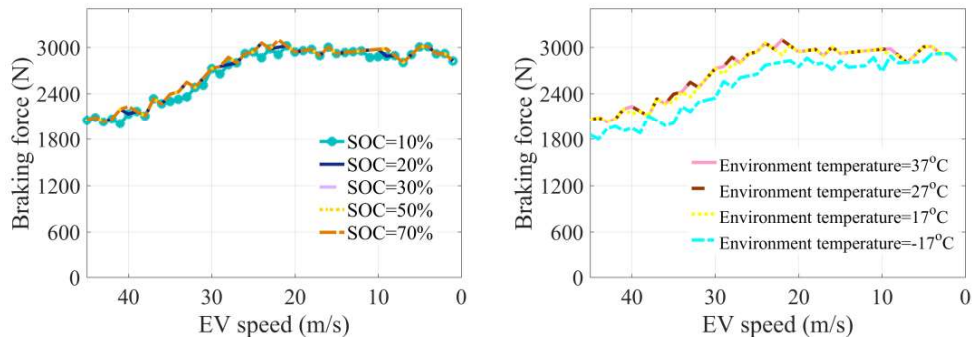


Fig. 14. Optimal output variable (CVT speed ratio and braking force) during the DM under different SOC and environment temperatures.

As shown in Fig. 14, the CVT speed ratio and braking force are inversely proportional to the EV speed. so when the EV is decelerating, the acceleration can remain almost unchanged due to the combined effect of braking force and wind resistance. The control of the output variable on the powertrain is manifested in that the braking force can determine the acceleration and input power of the EV, and the speed ratio of the CVT can adjust the efficiency of the whole powertrain.

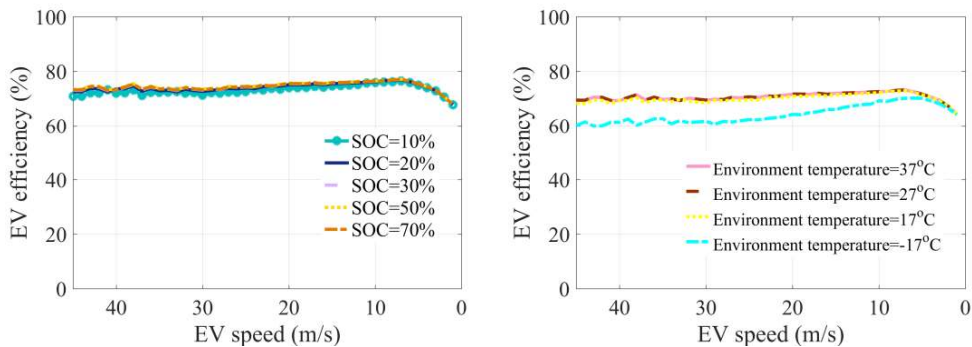


Fig. 15. EV efficiency during the DM under different SOC and environment temperatures.

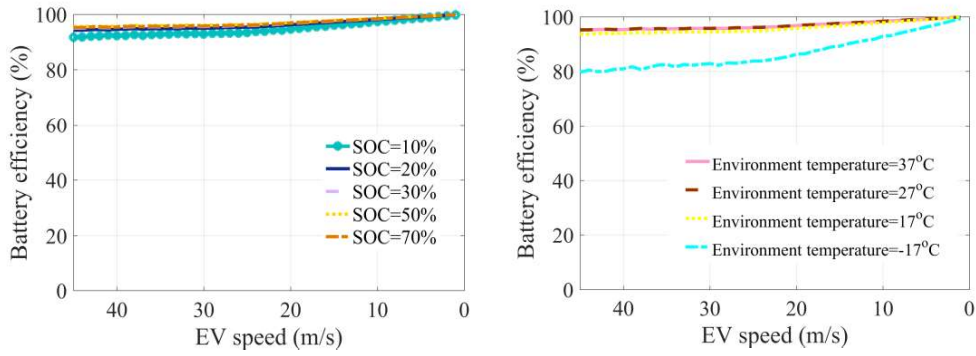


Fig. 16. Battery efficiency during the DM under different SOC and environment temperatures.

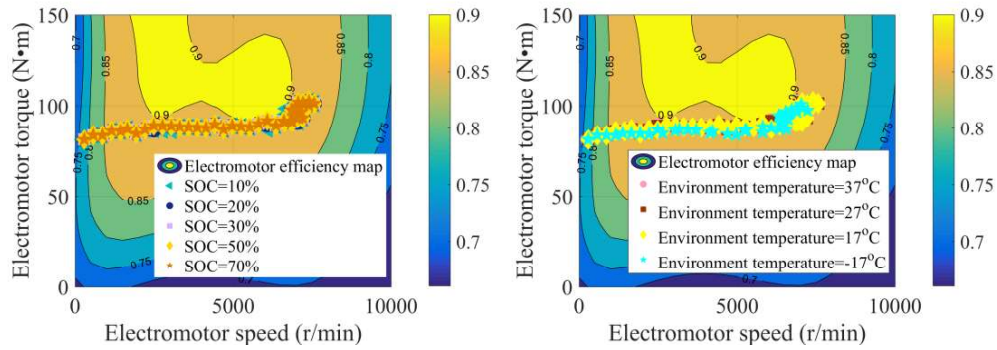


Fig. 17. Electromotor working state during the DM under different SOC and environment temperatures.

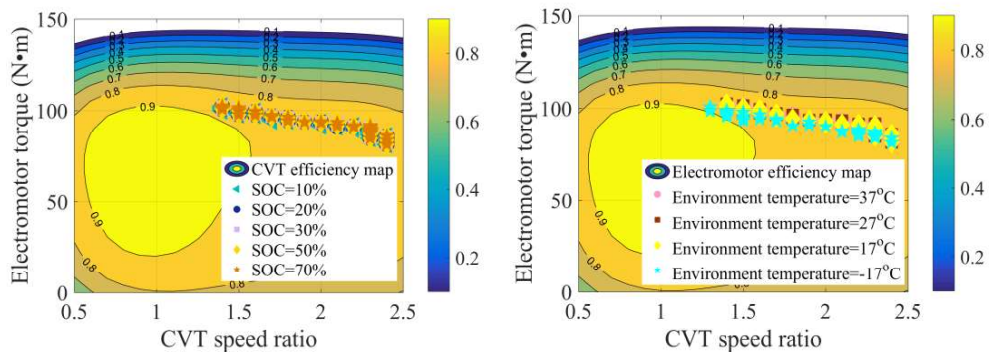


Fig. 18. CVT working state during the DM under different SOC and environment temperatures.

---

1 As shown in Figs. 15-18, each efficiency maintains a stable and high value reaching  
2  
3 at medium and high EV speeds (EV efficiency is around 78.8%, battery efficiency is  
4  
5 around 95.5%, electromotor efficiency is around 86.5%, and CVT efficacy is around  
6  
7 87.5%), while the efficiency of the electromotor and the EV drops rapidly at low EV  
8  
9 speeds (8.6m/s), which shows that the limitation of the electromotor still performs very  
10  
11 well during the deceleration process at low EV speeds. But, the battery performance at  
12  
13 low SOC no longer exhibits deterioration during the deceleration process, as the  
14  
15 battery's performance sensitivity under the low SOC becomes sluggish as the charge  
16  
17 internal resistance remains relatively unchanged. In addition, the electromotor's  
18  
19 limitation almost disappears during the deceleration process at high EV speed, which  
20  
21 is obviously different from the acceleration process. This because by controlling the  
22  
23 braking force at high EV speed, the rotational energy input to the powertrain during the  
24  
25 braking energy recovery process can be controlled, and through the adjustment of the  
26  
27 CVT, the electromotor speed can be maintained relatively unchanged, leading to the  
28  
29 electromotor high efficiency. Thus, it no longer shows the restriction of the electromotor  
30  
31 in high EV speed. As the EV speed continues to decrease, the speed ratio of the CVT  
32  
33 keeps increasing so as to keep the electromotor speed as large as possible. However,  
34  
35 according to Eq. (15), the decrease in EV speed cancels this effect, thus letting the  
36  
37 electromotor work in a low-efficiency area.  
38  
39  
40  
41  
42  
43  
44  
45  
46  
47  
48  
49  
50

#### 51 4.3 Eco-driving strategy feasibility during the UMM

52  
53 In the UMM simulation, the EV travels 100 kilometers at different EV speeds (EV  
54  
55 speed from 0m/s to 45m/s). In the first case, the initial SOC's are 20%, 30%, 50%, and  
56  
57  
58  
59  
60  
61  
62  
63  
64  
65

70% when the environment temperature is 27 °C . Besides, the environment temperatures are 37°C , 27°C . 17°C and -17°C when the initial SOC is 70% in the second case.

As shown in Fig. 19, compared with environment temperature, battery current is greatly affected by SOC. This is because the driving distance is long, and the SOC changes significantly, which deteriorates the battery's performance and then leads to the battery current correlation with driving distance and EV speed. Utterly different from battery current, the speed ratio of the CVT has always remained relatively stable around 1.25, only related to the EV speed, and the reason for this phenomenon can be found in the powertrain working state.

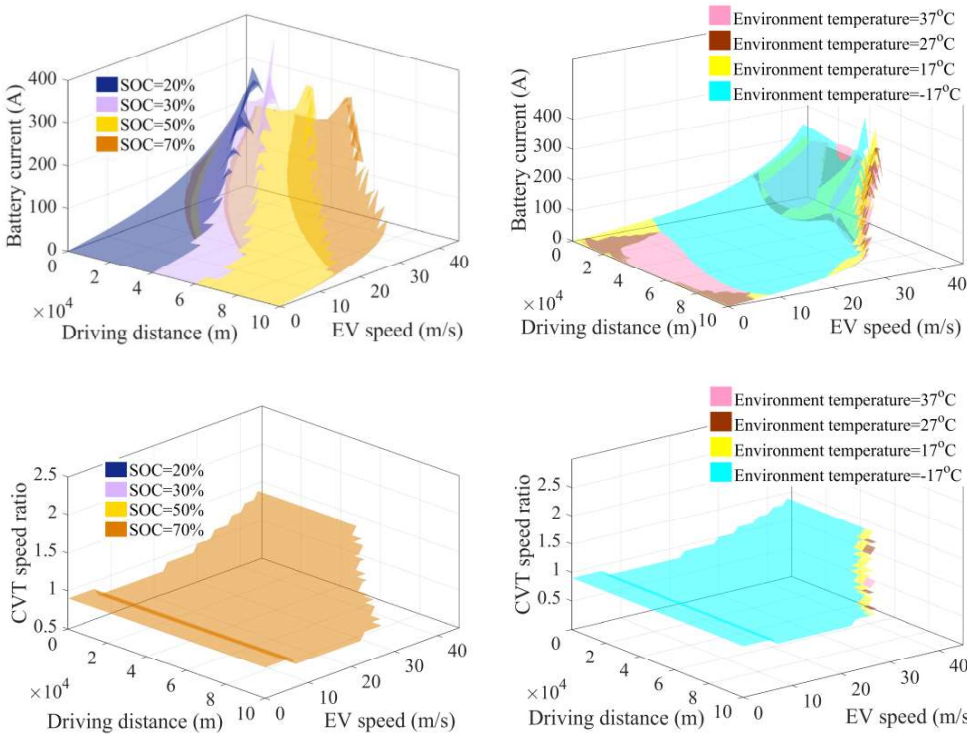


Fig. 19. Optimal output variable (battery current and CVT speed ratio) during the UMM under different SOC and environment temperatures.

As shown in Figs. 20-23, the various parts of the powertrain are only related to the EV speed and basically have nothing to do with SOC and environment temperature during the uniform motion process. However, when the EV travels at high speed for a long distance, the SOC becomes extremely low, so the battery's efficiency decreases significantly. In the process of uniform motion, the CVT can select the best speed ratio so that the electromotor can work in a high efficiency region of nearly 92.6%, and the electromotor does not show limitations except for the extremely low EV speed situation.

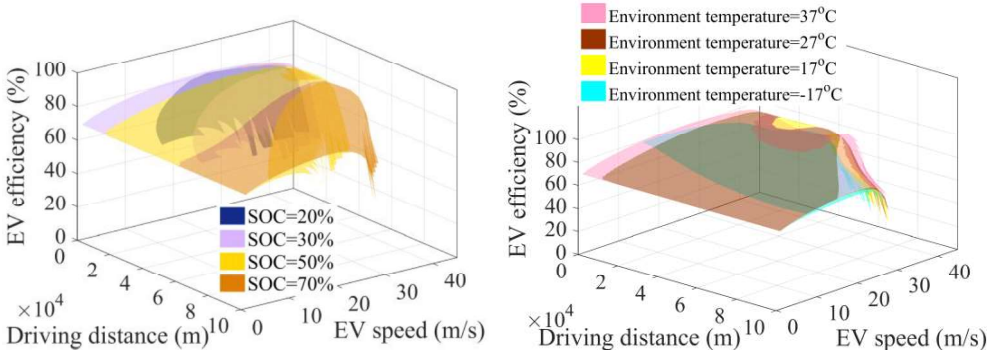


Fig. 20. EV efficiency during the UMM under different SOC and environment temperatures.

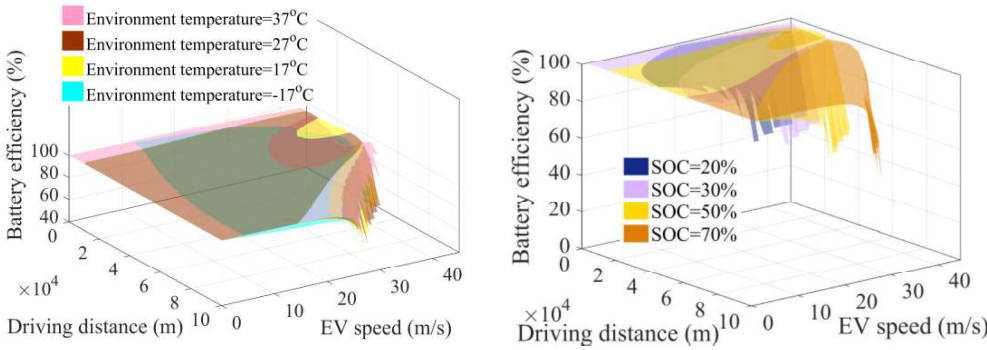


Fig. 21. Battery efficiency during the UMM under different SOC and environment temperatures.

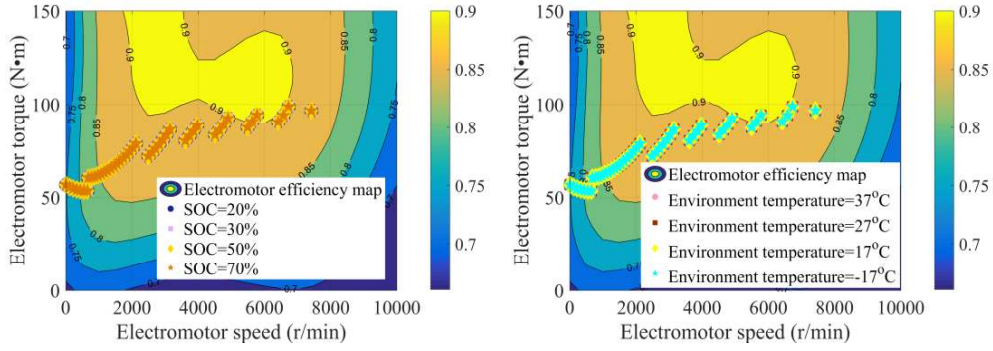


Fig. 22. Electromotor working state during the UMM under different SOC and environment temperatures.

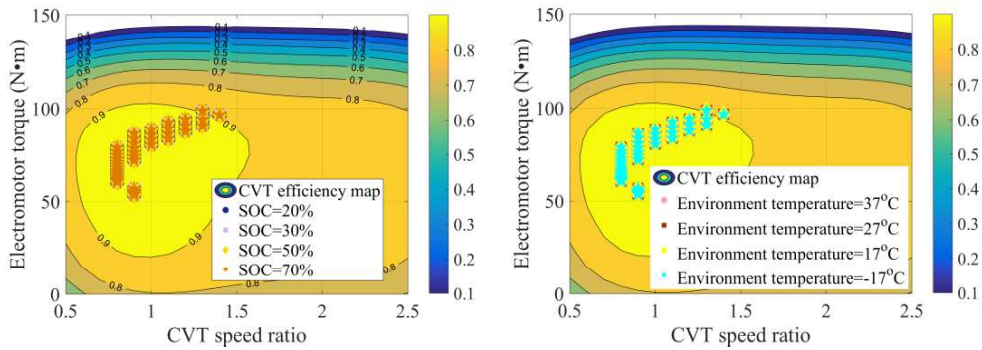


Fig. 23. CVT working state during the UMM under different SOC and environment temperatures.

#### 4.4 Eco-driving strategy adaptability under urban and suburban driving conditions

The proposed strategy for the three basic driving modes can coordinate the powertrain by adopting the best output variable corresponding to different EV speeds so as to realize the longest driving distance under the guarantee of the powertrain safety and driving comfort. Therefore, the proposed strategy has the potential to be applied in complex traffic situations. In order to verify the application of the strategy in realistic driving conditions, the proposed strategy is applied to urban and suburban driving conditions, respectively. Based on the speed-change of NEDC, the speed-change tasks

in urban and suburban driving conditions can be obtained, as NEDC is actually a test driving cycle including urban and suburban driving cycles. Here, the acceleration, deceleration, and uniform motion processes in the proposed strategy are used to replace the acceleration, deceleration, and uniform motion processes in NEDC, and the proposed strategy's performance under urban and suburban driving conditions is analyzed and discussed.

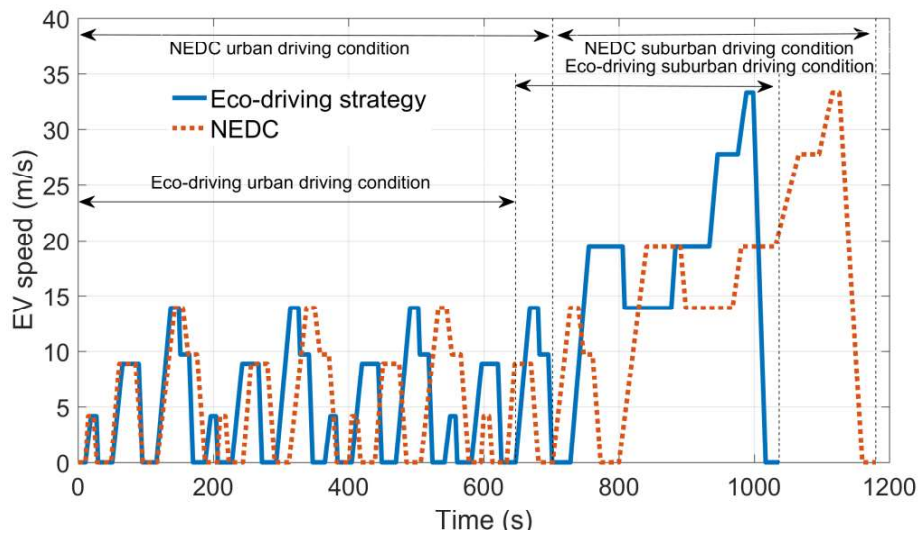
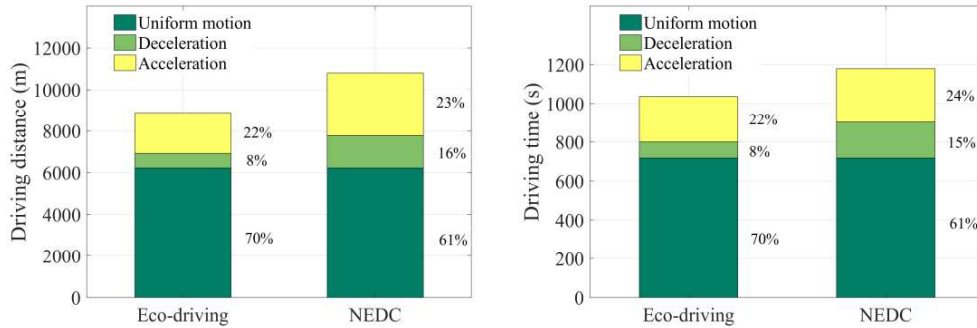


Fig. 24. The driving difference between NEDC and NEDC processed through the eco-driving strategy.

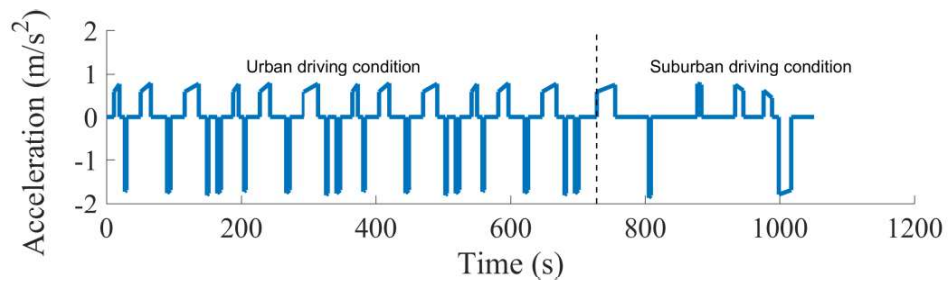
Fig. 24 shows the driving difference between NEDC and NEDC processed through the eco-driving strategy. After applying this strategy on NEDC, the distance and time required to complete the speed-change task are reduced by 17.13% and 12.12%. This is mainly because the acceleration's absolute value in the proposed strategy is larger than that in NEDC during the AM and DM. A more detailed result can be seen in Fig. 25. After applying this strategy, the proportion of the AM does not change significantly, while the proportion of DM is reduced from 16% to 8%, thereby increasing the

1 proportion of UMM from 61% to 70%. This shows that the proposed strategy's  
 2  
 3 acceleration and deceleration process can be well adapted to the realistic situation.  
 4  
 5  
 6



7  
 8  
 9  
 10  
 11  
 12  
 13  
 14  
 15  
 16  
 17  
 18  
 19  
 20 Fig. 25. Distance and time difference between NEDC and NEDC processed through  
 21  
 22 the eco-driving strategy.  
 23  
 24

25 To further explore the operation of the powertrain in realistic driving conditions,  
 26 the relevant variables are displayed in Figs. 26-30, including acceleration, braking force,  
 27 battery, electromotor, and CVT. It is found that all variables are changed within the  
 28 limited range, thus ensuring the safe operation of the powertrain and driving comfort.  
 29  
 30 However, due to the changes in the three driving modes, the optimal output variable  
 31 has abrupt changes, making the changes of relevant variables appear uneven.  
 32  
 33  
 34  
 35  
 36  
 37  
 38  
 39  
 40



41  
 42  
 43  
 44  
 45  
 46  
 47  
 48  
 49  
 50  
 51 Fig. 26. Acceleration of eco-driving strategy under urban and suburban driving  
 52  
 53 conditions.  
 54  
 55  
 56  
 57  
 58  
 59  
 60  
 61  
 62  
 63  
 64  
 65

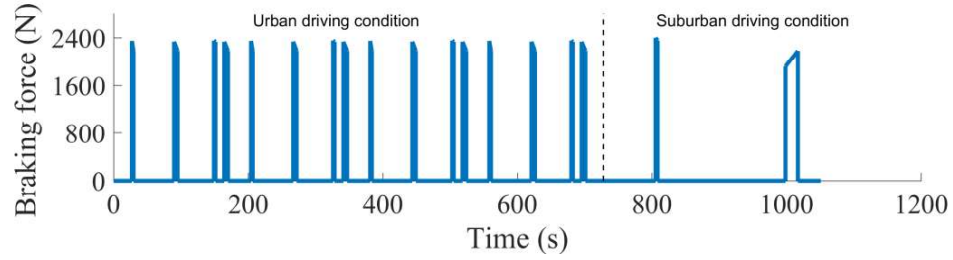
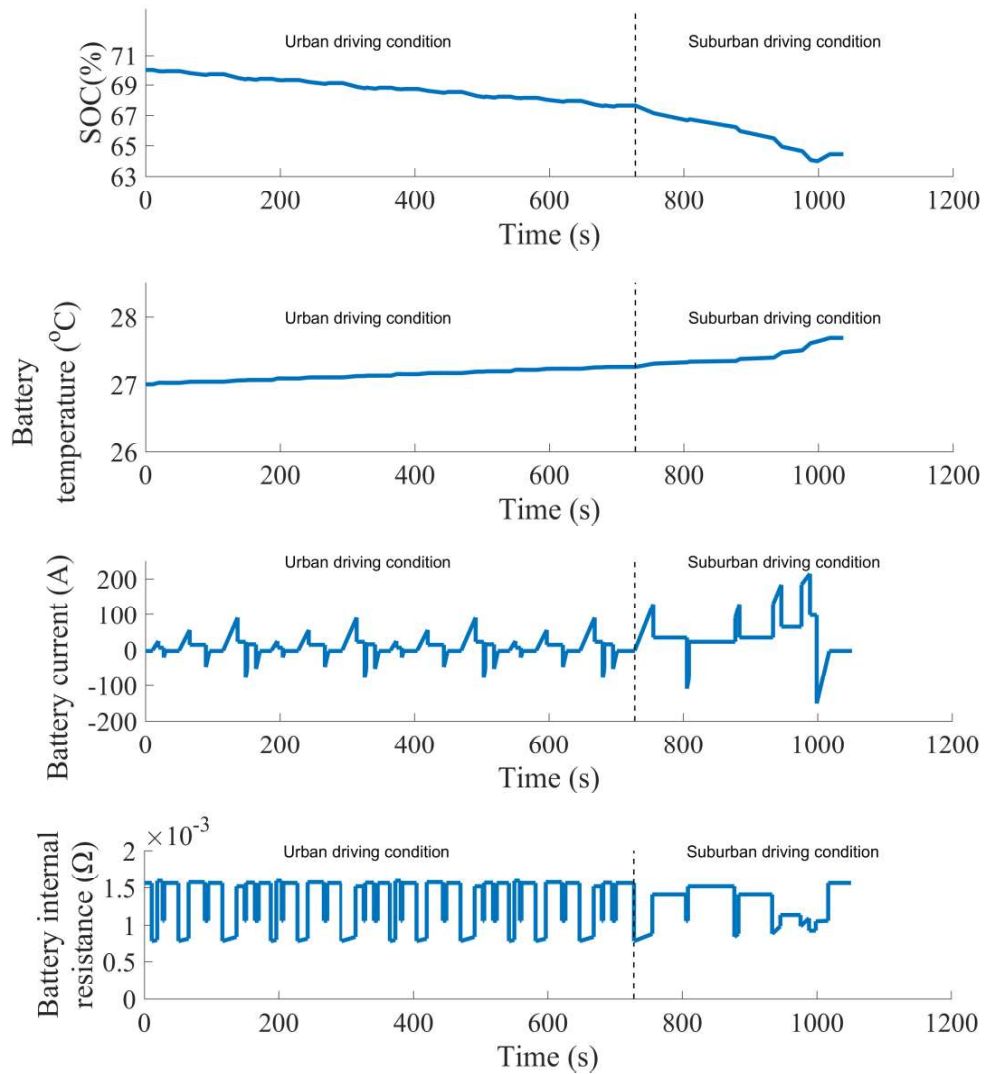


Fig. 27. Braking force of eco-driving strategy under urban and suburban driving conditions.



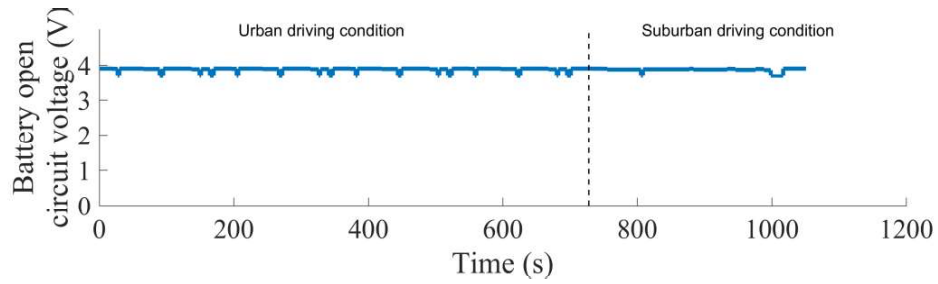


Fig. 28. Battery relevant variables of eco-driving strategy under urban and suburban driving conditions.

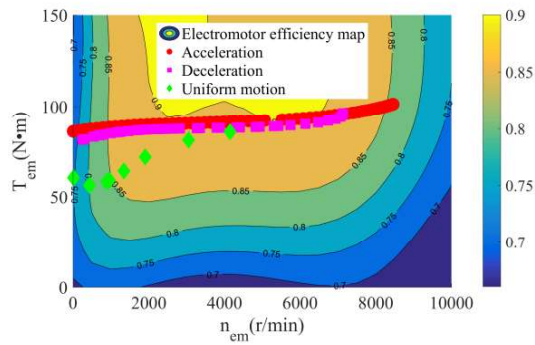
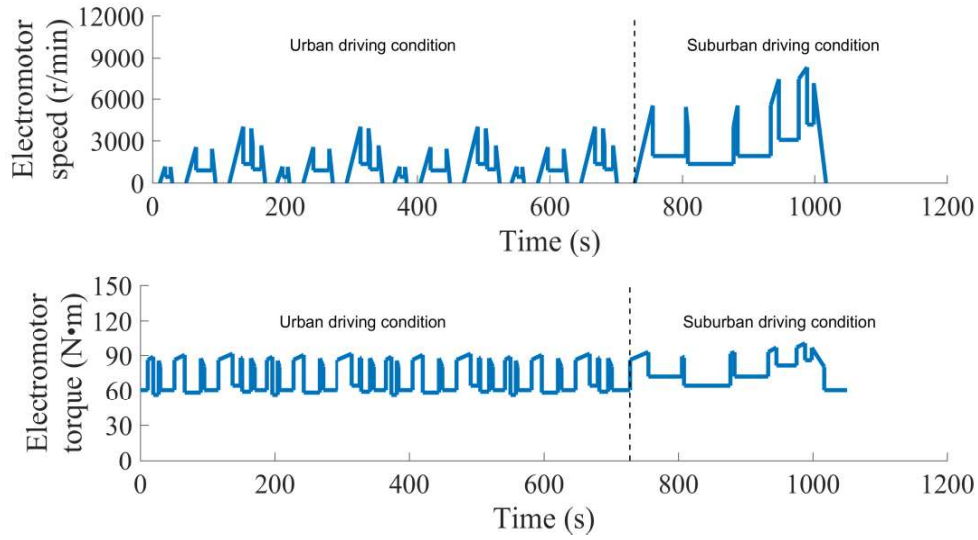


Fig. 29. Electromotor relevant variables of eco-driving strategy under urban and suburban driving conditions.

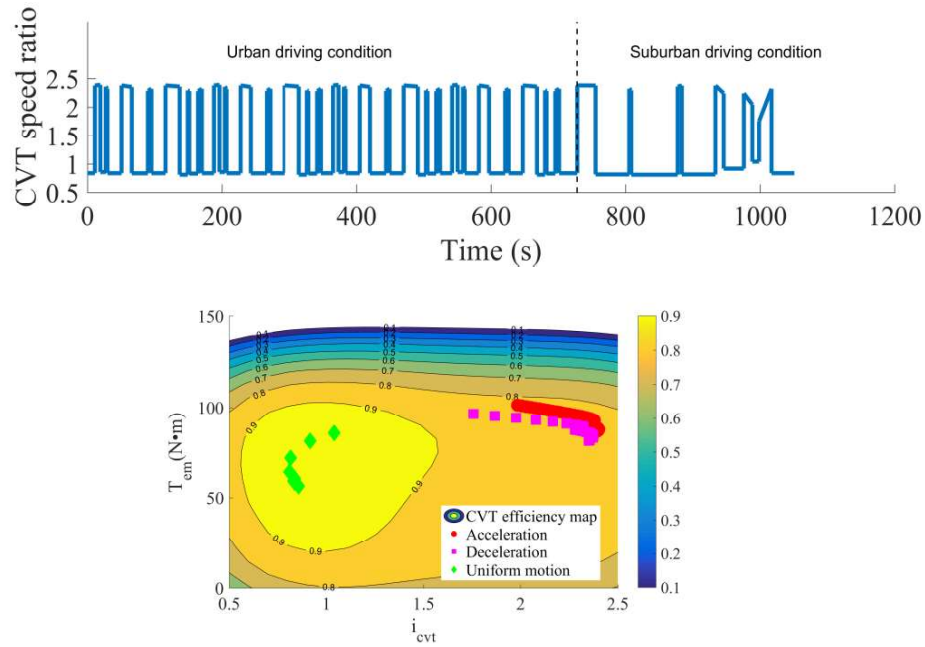
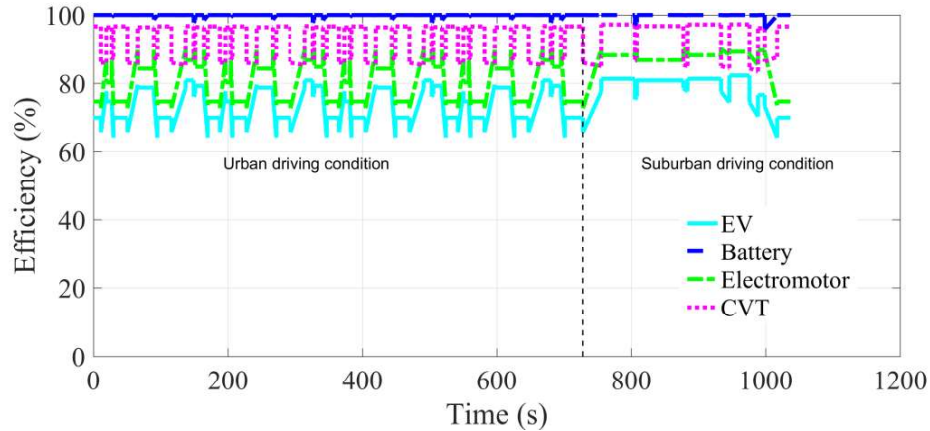


Fig. 30. CVT relevant variable of eco-driving strategy under urban and suburban driving conditions.

Fig. 31 shows the working state of each powertrain part is related to the driving mode because the direction of power flow changes with the driving mode. In AM and UMM, the power flows are in the forward direction, that is, energy is generated by the battery and is sequentially transmitted to the electromotor, CVT, and other transmission devices. In contrast, the power flow is in the reverse direction during the deceleration. In addition, there is a clear difference in the charge and discharge characteristics of the battery. In AM and UMM, the CVT sacrifices its efficiency, which is fluctuating from 85.3% to 96.7%, to adjust the electromotor working state so that the entire powertrain has higher efficiency which is fluctuating from 64% to 80.1%, reflecting the internal coupling effect of the powertrain. In contrast, in the process of uniform motion, the powertrain working state remains almost unchanged, and the CVT always works in the high-efficiency area, which can give full play to the regulating effect while losing very

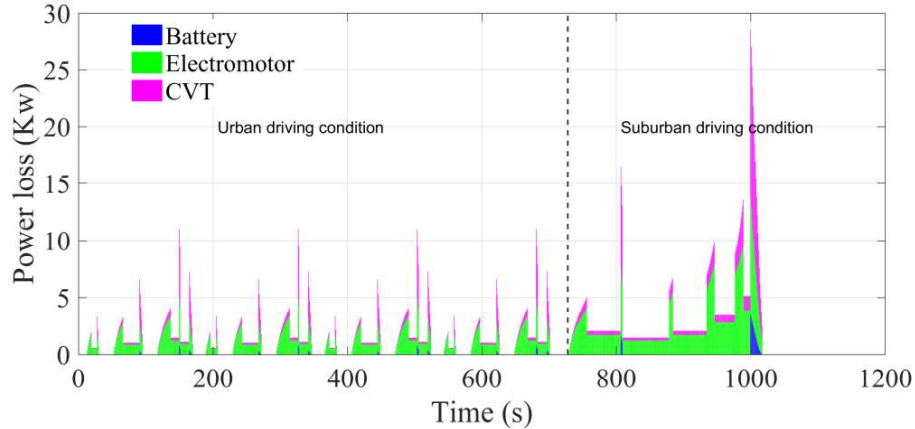
1 little energy. The powertrain working difference between urban and suburban driving  
2  
3 conditions is mainly caused by the EV speed difference, and the root cause is the  
4  
5  
6 electromotor limitation in low and high EV speeds.  
7  
8



9  
10  
11  
12  
13  
14  
15  
16  
17  
18  
19  
20  
21  
22  
23  
24  
25  
26  
27  
28  
29  
30  
31  
32  
33  
34  
35  
36  
37  
38  
39  
40  
41  
42  
43  
44  
45  
46  
47  
48  
49  
50  
51  
52  
53  
54  
55  
56  
57  
58  
59  
60  
61  
62  
63  
64  
65  
Fig. 31. Efficiency contrast of eco-driving strategy under urban and suburban driving conditions.

To better analyze the power loss, Fig. 32 shows the specific power loss of each powertrain part. It is worth noting that the battery can adapt well to both of the driving conditions, as the SOC and environment temperature always keep normal. As for the electromotor, it usually accounts for most of the power loss, fluctuating from 1.1kw to 13.2kw. Although the CVT has high efficiency, which is nearly 85.3%, in the deceleration process, as a device directly connected to the input energy, it still loses most of the power, maximum to 26.9kw when the EV speed reaches 34m/s, and the loss increases significantly with the increase in EV speed. Therefore, most of the efficiency loss of EV is caused by the electromotor. Through the coupling effect of the powertrain, the CVT can play a regulating role, thereby alleviating the electromotor's limitation at low and high EV speeds. Besides, the EV loses the lowest power during the uniform

1 motion and has the best economic efficiency, while the deceleration process is the  
 2 process in which the EV loses the most power, and the economic efficiency is poorest,  
 3 especially in high EV speed driving condition.  
 4  
 5  
 6  
 7  
 8



9  
 10  
 11  
 12  
 13  
 14  
 15  
 16  
 17  
 18  
 19  
 20  
 21  
 22  
 23  
 24  
 25  
 26  
 27  
 28  
 29  
 30  
 31  
 32  
 33  
 34  
 35  
 36  
 37  
 38  
 39  
 40  
 41  
 42  
 43  
 44  
 45  
 46  
 47  
 48  
 49  
 50  
 51  
 52  
 53  
 54  
 55  
 56  
 57  
 58  
 59  
 60  
 61  
 62  
 63  
 64  
 65

Fig. 32. Power loss contrast of eco-driving strategy under urban and suburban driving conditions.

Obviously, due to the different speed-change tasks in urban and suburban driving conditions, the control variables of the powertrain in different driving modes are significantly different, resulting in different average accelerations and powertrain working state. The adopted acceleration in different driving modes under urban and suburban driving conditions will produce different driving distances and times. Table 3 shows the difference in driving distance and time of different driving modes under urban and suburban driving conditions. The UMM is the most crucial part in urban and suburban driving conditions, which is almost bigger than 67%, while the DM is the least proportioned part, which is less than 9%. It is worth noting that the proportions of AM and DM in urban driving condition are larger than that in suburban driving condition, while the proportions of UMM are the opposite. So, the proportions of

different driving modes in both driving conditions have the same order, i.e., uniform motion process > acceleration process > deceleration process.

**Table 3** Distance and time of driving modes under different driving conditions.

Driving condition		Urban driving condition			Suburban driving condition		
		AM	DM	UMM	AM	DM	UMM
Distance	Value (m)	738.78	282.08	2158.89	922.94	342.68	4069.44
	Proportion (%)	23.23	8.87	67.90	17.30	6.42	76.28
Time	Value (s)	176	64	489	59	22	231
	Proportion (%)	24.14	8.78	67.08	18.91	7.05	74.04

As the powertrain's energy supply device, the change of SOC and battery temperature is the main manifestation of the powertrain working state and can well reflect the performance of the strategy in urban and suburban driving conditions. The smaller the SOC and battery temperature changes, indicating that the longer the EV driving range and the better the stability of battery performance. The proposed strategy's performance can be obtained according to the SOC and battery temperature changes per meter in different basic driving modes (Table 4). UMM has a better performance than AM and DM in terms of SOC and battery change per meter, as the values caused by UMM are much lower. Besides, compared with the suburban driving condition, AM and DM respectively decelerates 36% and increases 50% in terms of SOC change per meter, and decelerates 36.84% and 70.59% in terms of battery

temperature change per meter. In contrast, UMM increases 20% and 133.33% in terms of SOC and battery temperature change per meter, respectively. Therefore, in terms of SOC change, AM and DM are more suitable for urban driving conditions, and UMM is more suitable for suburban driving condition. As for the change of battery temperature, the driving mode adaptability is consistent with SOC change. After comparing Tables 3 and 4, the proportion of different driving modes in urban and suburban driving conditions can almost match the applicability preference of the corresponding strategies, as the UMM is the most crucial part in urban and suburban driving conditions (at least occupies 67.08%), as well as possess the most excellent performance in the change of SOC and battery temperature.

**Table 4** Strategy applicability of driving modes under different driving conditions.

Driving condition	Urban driving condition			Suburban driving condition		
	AM	DM	UMM	AM	DM	UMM
Average speed (m/s)	5.24	4.41	4.42	12.42	15.58	17.62
SOC change per meter ( $\times 10^{-2}$ %/m)	0.16	0.21	0.06	0.25	0.14	0.05
Battery temperature change per meter ( $\times 10^{-3}$ °C/m)	0.24	0.05	0.07	0.38	0.17	0.03

#### 4.5 Reflections based on the eco-driving strategy feasibility and adaptability

Considering the above simulation and discussion, the proposed driving strategy can make full use of the internal coupling effect of the EV powertrain through the adjustment effect of the CVT, so as to eliminate parts of negative effects caused by the

---

1 battery degradation and the limitation of the electromotor. In this paper, models are  
2  
3 constructed based on the numerical relationship between the input and output of each  
4  
5 component of the powertrain, and the numerical solution of the proposed strategy is  
6  
7 solved. Although each powertrain component used in different types of EVs is  
8  
9 heterogeneous, the changing trend of the numerical relationship between the input and  
10  
11 output is consistent. Therefore, the influence of the numerical characteristics of each  
12  
13 component on the EV can be explored through the simulation results. Here, some  
14  
15 reflections on EV energy performance, powertrain optimization potential, and EV  
16  
17 optimization guidelines are conducted based on sections 4.1-4.4.  
18  
19  
20  
21  
22  
23

24  
25 Sections 4.1-4.3 can provide a good basis for the study of EV energy performance  
26  
27 and the powertrain optimization potential. As far as EV energy performance is  
28  
29 concerned, changes in EV energy performance will affect the EV economy performance  
30  
31 and power performance. The specific manifestation is that changes in the relationship  
32  
33 between battery input and battery output will affect EV efficiency and acceleration.  
34  
35 When the power flow in the forward direction, that is, AM and UMM, the EV energy  
36  
37 performance is less affected by environment temperature change, but is more affected  
38  
39 by SOC change. In the vast majority of SOC (10%-100%), the EV energy performance  
40  
41 has strong stability, which shows that the change of SOC and environment temperature  
42  
43 will not interfere with the EV economy performance and power performance. However,  
44  
45 when the SOC is low (0%-10%), due to the rapid decrease of the battery open circuit  
46  
47 voltage and the dramatic increase of the battery discharge internal resistance, the battery  
48  
49 working state will deteriorate, showing the battery degradation, thereby reducing the  
50  
51  
52  
53  
54  
55  
56  
57  
58  
59  
60  
61  
62  
63  
64  
65

---

1 EV economy performance and power performance. The intuitive manifestation of the  
2  
3 economic performance decline is that in the AM when the EV speed is 35.1m/s and the  
4  
5 SOC drops from 20% to 10%, the EV efficiency drops from 55.88% to 37.37%, a 33.12%  
6  
7 drop. The intuitive manifestation of the decline in power performance is that in AM  
8  
9 when the EV speed is 16.1m/s and the SOC drops from 20% to 10%, the acceleration  
10  
11 drops from 0.8 m<sup>2</sup>/s to 0.25 m<sup>2</sup>/s, a 68.75% drop. When the power flows in the reverse  
12  
13 direction, that is DM, the EV energy performance has nothing to do with the change of  
14  
15 SOC, but is greatly affected by the low environment temperature (-17 °C). Under most  
16  
17 environment temperatures (17 °C -37 °C), the EV energy performance has strong  
18  
19 stability, but when the environment temperature is low (-17 °C), the energy  
20  
21 performance is no longer stable due to the increase in the battery charge internal  
22  
23 resistance.  
24  
25  
26  
27  
28  
29  
30  
31

32  
33 According to the powertrain working state in each driving mode, the powertrain  
34  
35 optimization potential can be analyzed. The powertrain optimization potential is  
36  
37 possibly carried out from two aspects. The first is to improve the self-performance of  
38  
39 the battery, the electromotor, and the CVT, and the second is to optimize the utilization  
40  
41 requirements according to the working states. As an energy supply device, the battery  
42  
43 degradation under low SOC (0%-10%) will greatly reduce the EV economy  
44  
45 performance and power performance in AM and UMM. Therefore, in addition to  
46  
47 reducing the impact of SOC on battery performance, reasonable planning of EV driving  
48  
49 mileage, the selection of an appropriate charging scheme, and the choice of a route  
50  
51 considering the road slope can also effectively improve the EV energy performance.  
52  
53  
54  
55  
56  
57  
58  
59  
60

---

1 The limitation of electromotor at high and low electromotor speed is the main factor  
2  
3 restricting EV economy performance and power performance. Even though with the  
4  
5 help of the CVT adjustment effect, the electromotor still exhibits inefficiency at high  
6  
7 and low EV speed in AM and UMM, and inefficiency at low EV speed in DM.  
8  
9 Therefore, in addition to improving the electromotor efficiency at high and low  
10  
11 electromotor speed, optimizing the task of EV speed change, i.e., reducing the time at  
12  
13 high and low EV speed in AM and UMM, and the time at low EV speed in DM, can  
14  
15 also effectively improve the utilization of EV energy. The CVT limited adjustment  
16  
17 effect at high EV speed in AM and UMM is consistent with the electromotor limited  
18  
19 performance, as well as the CVT limited adjustment effect at low EV speed in DM.  
20  
21 Therefore, in addition to increasing the maximum CVT speed ratio, optimizing the task  
22  
23 of EV speed change is also applicable to CVT.  
24  
25  
26  
27  
28  
29  
30  
31  
32

33 From section 4.4, it is possible to conclude EV optimization guidelines according  
34  
35 to the realistic driving conditions. First, the discontinuity of the powertrain control  
36  
37 variables caused by the driving mode change will produce sudden changes in  
38  
39 acceleration, thereby affecting the driver's comfort and producing a stop-and-go  
40  
41 phenomenon. Thus, EVs with continuous powertrain control variables will be more  
42  
43 adapted to realistic driving conditions. Furthermore, due to the distinct differences in  
44  
45 the proportions of different driving modes under realistic driving conditions, the  
46  
47 proportions of UMM, AM, and DM can be used as weights to execute differential  
48  
49 optimization of EV performance in different driving modes when the investing cost in  
50  
51  
52  
53  
54  
55  
56  
57  
58  
59  
60  
61  
62  
63  
64  
65

---

EV optimization is limited, so as to ensure the maximum utilization of the EV optimization potential.

## 5. Conclusions

In summary, there is an urgent need to develop an eco-driving strategy that can maximize the EV driving range and be widely used according to specific speed-change tasks under realistic driving conditions. In this paper, the maximum driving range is enhanced by different adopted acceleration and powertrain coupling effect considering the entire powertrain efficiency and the battery thermal effect. Besides, the comprehensive application is guaranteed by the strategy insensitivity to SOC and environment temperature, as well as the consistency of driving mode proportion and applicability preference in both the urban and suburban driving conditions.

In the simulation and discussion, the correlation between the proposed strategies used in different driving modes and the powertrain working state are discussed in-depth. The results show that the proposed strategy applied to different driving modes can make full use of the internal coupling effect of the powertrain, sacrificing CVT efficiency to alleviate the electromotor efficiency decline and the battery performance deterioration, so as to achieve the highest EV efficiency. But, once the SOC lower than 10%, the powertrain will be drastically disturbed, reducing acceleration and EV efficiency up to 68.78% and 33.12% in the acceleration process, respectively. Meanwhile, the proposed strategy can significantly shorten the deceleration proportion from 16% to 8% once the proposed strategy is adopted in NEDC, thereby increasing the uniform motion proportion from 61% to 70%. However, the driving mode proportions in both driving

---

1 conditions have the same order, i.e., uniform motion process > acceleration process >  
2  
3 deceleration process. And this is consistent with the strategy applicability of driving  
4  
5  
6 modes, where the uniform motion possesses a better performance than other driving  
7  
8  
9 processes in terms of SOC and battery change. In addition, compared with the suburban  
10  
11 driving condition, acceleration and deceleration processes perform better in urban  
12  
13 driving condition while the uniform motion driving process is the opposite. The  
14  
15 applicability preference can be illustrated by the changes per meter in SOC and battery  
16  
17 temperature. Because these changes from urban driving condition to suburban driving  
18  
19 condition respectively decelerate 36% and 36.84% in the acceleration process, and -50%  
20  
21 and 70.59% in the deceleration process. On the contrary, these changes increase 20%  
22  
23 and 133.33% in the uniform motion process, respectively. In the future, more in-depth  
24  
25 researches will be executed to verify the strategy by more detailed and realistic data,  
26  
27 and make the powertrain better adapt to different driving conditions, including the  
28  
29 improvement of the inefficiency of electromotor at high and low EV speeds, and the  
30  
31 deterioration of battery performance at low SOC.  
32  
33  
34  
35  
36  
37  
38  
39  
40

## 41 **Acknowledgment**

42 We are grateful for the anonymous referees' valuable comments and suggestions.  
43  
44  
45 This work was supported by the National Natural Science Foundation of China  
46  
47 (71890971; 71890970), Royal Academy of Engineering Newton Fund (Project  
48  
49 TSPC1025), and the Academic Excellence Foundation of BUAA for Ph.D. Students  
50  
51 (202159).  
52  
53  
54  
55  
56  
57

## 58 **Appendix**

**Table 1** The relevant values of the fitting function  $U_{oc}$ .

Parameter	Value	Parameter	Value
$A_{00}^{OC}$	3.435	$A_{12}^{OC}$	$-2.917 \times 10^{-5}$
$A_{01}^{OC}$	0.006806	$A_{13}^{OC}$	$2.961 \times 10^{-7}$
$A_{02}^{OC}$	-0.000318	$A_{14}^{OC}$	$-1.046 \times 10^{-9}$
$A_{03}^{OC}$	$8.722 \times 10^{-6}$	$A_{20}^{OC}$	0.0002904
$A_{04}^{OC}$	$-9.383 \times 10^{-8}$	$A_{21}^{OC}$	$-1.449 \times 10^{-5}$
$A_{05}^{OC}$	$3.623 \times 10^{-10}$	$A_{22}^{OC}$	$2.513 \times 10^{-7}$
$A_{10}^{OC}$	-0.0194	$A_{23}^{OC}$	$-1.363 \times 10^{-9}$
$A_{11}^{OC}$	0.0012		
$N_{OC}^1$	2	$N_{OC}^2$	5

**Table 2** The relevant values of the fitting function  $r_{discharge}$ .

Parameter	Value	Parameter	Value
$A_{00}^{discharge}$	0.008904	$A_{12}^{discharge}$	$1.295 \times 10^{-6}$
$A_{01}^{discharge}$	-0.0006419	$A_{13}^{discharge}$	$-1.193 \times 10^{-8}$
$A_{02}^{discharge}$	$3.239 \times 10^{-5}$	$A_{14}^{discharge}$	$3.532 \times 10^{-11}$
$A_{03}^{discharge}$	$-7.703 \times 10^{-7}$	$A_{20}^{discharge}$	$-9.228 \times 10^{-6}$
$A_{04}^{discharge}$	$8.188 \times 10^{-9}$	$A_{21}^{discharge}$	$8.877 \times 10^{-7}$
$A_{05}^{discharge}$	$-3.139 \times 10^{-11}$	$A_{22}^{discharge}$	$-1.75 \times 10^{-8}$
$A_{10}^{discharge}$	0.0004291	$A_{23}^{discharge}$	$9.84 \times 10^{-11}$
$A_{11}^{discharge}$	$-5.15 \times 10^{-5}$		
$N_{discharge}^1$	2	$N_{discharge}^2$	5

**Table 3** The relevant values of the fitting function  $r_{\text{charge}}$ .

Parameter	Value	Parameter	Value
$A_{00}^{\text{charge}}$	0.004791	$A_{12}^{\text{charge}}$	$1.626 \times 10^{-7}$
$A_{01}^{\text{charge}}$	-0.000105	$A_{13}^{\text{charge}}$	$-9.579 \times 10^{-10}$
$A_{02}^{\text{charge}}$	$5.256 \times 10^{-6}$	$A_{14}^{\text{charge}}$	$-1.794 \times 10^{-13}$
$A_{03}^{\text{charge}}$	$-1.329 \times 10^{-7}$	$A_{20}^{\text{charge}}$	$1.486 \times 10^{-6}$
$A_{04}^{\text{charge}}$	$1.438 \times 10^{-9}$	$A_{21}^{\text{charge}}$	$1.594 \times 10^{-7}$
$A_{05}^{\text{charge}}$	$-5.436e \times 10^{-12}$	$A_{22}^{\text{charge}}$	$-3.705 \times 10^{-9}$
$A_{10}^{\text{charge}}$	-0.0001185	$A_{23}^{\text{charge}}$	$2.185 \times 10^{-11}$
$A_{11}^{\text{charge}}$	$-6.717 \times 10^{-6}$		
$N_{\text{charge}}^1$	2	$N_{\text{charge}}^2$	5

**Table 4** The relevant values of the fitting function  $\eta_{\text{em}}$ .

Parameter	Value	Parameter	Value
$A_{00}^{\text{em}}$	0.6882	$A_{21}^{\text{em}}$	$-4.833 \times 10^{-10}$
$A_{01}^{\text{em}}$	0.002532	$A_{22}^{\text{em}}$	$1.021 \times 10^{-12}$
$A_{02}^{\text{em}}$	$-2.754 \times 10^{-5}$	$A_{23}^{\text{em}}$	$-1.604 \times 10^{-15}$
$A_{03}^{\text{em}}$	$-5.721 \times 10^{-8}$	$A_{30}^{\text{em}}$	$1.595 \times 10^{-11}$
$A_{04}^{\text{em}}$	$-1.182 \times 10^{-8}$	$A_{31}^{\text{em}}$	$4.54 \times 10^{-14}$
$A_{05}^{\text{em}}$	$-3.938 \times 10^{-12}$	$A_{32}^{\text{em}}$	$-9.771 \times 10^{-18}$
$A_{10}^{\text{em}}$	$7.09 \times 10^{-5}$	$A_{40}^{\text{em}}$	$-1.733 \times 10^{-15}$
$A_{11}^{\text{em}}$	$1.799 \times 10^{-6}$	$A_{41}^{\text{em}}$	$-1.936 \times 10^{-18}$
$A_{20}^{\text{em}}$	$-5.922 \times 10^{-8}$	$A_{50}^{\text{em}}$	$6.578 \times 10^{-29}$

$N_{em}^1$	5	$N_{em}^2$	5
------------	---	------------	---

**Table 5** The relevant values of the fitting function  $\eta_{cvt}$ .

Parameter	Value	Parameter	Value
$A_{00}^{cvt}$	-0.1833	$A_{13}^{cvt}$	$2.778 \times 10^{-8}$
$A_{01}^{cvt}$	0.01414	$A_{20}^{cvt}$	-2.598
$A_{02}^{cvt}$	-0.0002416	$A_{21}^{cvt}$	0.001959
$A_{03}^{cvt}$	$2.371 \times 10^{-6}$	$A_{22}^{cvt}$	$-2.279 \times 10^{-5}$
$A_{04}^{cvt}$	$-1.182 \times 10^{-8}$	$A_{30}^{cvt}$	1.072
$A_{10}^{cvt}$	2.666	$A_{31}^{cvt}$	0.0001476
$A_{11}^{cvt}$	-0.008035	$A_{40}^{cvt}$	-0.1613
$A_{12}^{cvt}$	$7.294 \times 10^{-5}$		
$N_{cvt}^1$	4	$N_{cvt}^2$	4

**Table 6** The EV related parameters.

Parameter	Value	Parameter	Value
$M$	1600kg	$\delta$	1.2
$C_A$	0.43 kg/m	$g$	9.8m/s <sup>2</sup>
$f$	0.028	$r$	0.307 m
$i_o$	3.863	$u_{max}$	45 m/s
$a_{min}$	-2 m/s <sup>2</sup>	$a_{max}$	3 m/s <sup>2</sup>
$i_{cvtmin}$	0.5	$i_{cvtmax}$	2.5
$T_{emmin}$	0 Nm	$T_{emmax}$	150 Nm
$I_{min}$	-100A	$I_{max}$	280A

1  
2  
3  
4  
5  
6  
7  
8  
9  
10  
11  
12  
13  
14  
15  
16  
17  
18  
19  
20  
21  
22  
23  
24  
25  
26  
27  
28  
29  
30  
31  
32  
33  
34  
35  
36  
37  
38  
39  
40  
41  
42  
43  
44  
45  
46  
47  
48  
49  
50  
51  
52  
53  
54  
55  
56  
57  
58  
59  
60  
61  
62  
63  
64  
65

---

$\eta_t$	0.95	$\mu$	0.7
$n_{\text{cell}}$	110	$C_{\text{battery}}$	100 Ah
$m_{\text{battery}}$	385 kg	$c_{\text{battery}}$	1062.2 Jkg <sup>-1</sup> K <sup>-1</sup>
$\alpha$	5 W/(m <sup>2</sup> K)	$S_{\text{battery}}$	118874 mm <sup>2</sup>
$T_{\text{environment}}$	27°C		

---

**Table 7** The simulation parameters.

---

Parameter	Value	Parameter	Value
$N$	180	$k$	200
$m$	2000	$x$	500
$Z$	1000		

---

**References**

[1] Guo D, Zhou C. Potential performance analysis and future trend prediction of electric vehicle with V2G/V2H/V2B capability. *AIMS Energy* 2016;4(22):331-46.

[2] Li J, Jin X, Xiong R. Multi-objective optimization study of energy management strategy and economic analysis for a range-extended electric bus. *Appl Energy* 2017;194:798-807.

[3] Guo L, Gao B, Gao Y, Chen H. Optimal energy management for HEVs in eco-driving applications using bi-level MPC. *IEEE Trans Intell Transp Syst* 2016;18(8):2153-62.

[4] Ershad NF, Mehrjardi RT, Ehsani M. Electro-mechanical EV powertrain with reduced volt-ampere rating. *IEEE Trans Veh Technol* 2018;68(1):224-33.

- 
- 1 [5] Song Z, Li J, Han X, Xu L, Lu L, Ouyang M, Hofmann H. Multi-objective  
2  
3 optimization of a semi-active battery/supercapacitor energy storage system for electric  
4  
5 vehicles. *Appl Energy* 2014;135:212-224.  
6  
7  
8  
9 [6] Saerens B, Bulck EVD. Calculation of the minimum-fuel driving control based on  
10  
11 pontryagin's maximum principle. *Transp Res Part D* 2013;24:89-97.  
12  
13  
14 [7] Wu J, Wei Z, Liu K, Quan Z, Li Y. Battery-involved energy management for hybrid  
15  
16 electric bus based on expert-assistance deep deterministic policy gradient algorithm.  
17  
18 *IEEE Trans Veh Technol* 2020, 69(11): 12786-12796.  
19  
20  
21 [8] Huang Y, Ng EC, Zhou JL, Surawski NC, Chan EF, Hong G. Eco-driving  
22  
23 technology for sustainable road transport: A review. *Renew Sust Energ Rev*  
24  
25  
26  
27  
28 2018;93:596-609.  
29  
30  
31 [9] Zhang C, Allafi W, Dinh Q, Ascencio P, Marco J. Online estimation of battery  
32  
33 equivalent circuit model parameters and state of charge using decoupled least squares  
34  
35 technique. *Energy* 2018;142:678-88.  
36  
37  
38  
39 [10] Sun F, Xiong R, He H, Li W, Aussems JEE. Model-based dynamic multi-parameter  
40  
41 method for peak power estimation of lithium-ion batteries. *Appl Energy* 2012;96:378-  
42  
43  
44  
45 86.  
46  
47  
48 [11] He H, Xiong R, Guo H. Online estimation of model parameters and state-of-charge  
49  
50 of LiFePO<sub>4</sub> batteries in electric vehicles. *Appl Energy* 2012;89(1):413-20.  
51  
52  
53 [12] Song Z, Hofmann H, Li J, Han X, Ouyang M. Optimization for a hybrid energy  
54  
55 storage system in electric vehicles using dynamic programming approach. *Appl Energy*  
56  
57  
58 2015;139:151-62.  
59  
60  
61  
62  
63  
64  
65

---

1 [13] Wei Z, Zhao J, He H, Ding G, Cui H, Liu L. Future smart battery and management:  
2  
3 Advanced sensing from external to embedded multi-dimensional measurement. J.  
4  
5 Power Sources 2021;489:229462.  
6  
7

8  
9 [14] Lu J, Lin C, Chen Q. Comparison study of 3 types of battery models for electrical  
10  
11 vehicle. Chinese J. Power Sources 2006;7:535-8.  
12  
13

14 [15] Widanage WD, Barai A, Chouchelamane GH, Uddin K, McGordon A, Marco J,  
15  
16 Jennings P. Design and use of multisine signals for Li-ion battery equivalent circuit  
17  
18 modelling. Part 2: Model estimation. J. Power Sources 2016;324:61-9.  
19  
20  
21

22 [16] Wei Z, Zhao J, Ji D, Tseng KJ. A multi-timescale estimator for battery state of  
23  
24 charge and capacity dual estimation based on an online identified model. Appl Energy  
25  
26 2017;204:1264-74.  
27  
28  
29

30 [17] Li J, Wang L, Lyu C, Pecht M. State of charge estimation based on a simplified  
31  
32 electrochemical model for a single LiCoO<sub>2</sub> battery and battery pack. Energy  
33  
34 2017;133:572-83.  
35  
36  
37

38 [18] Zeraoulia M, Benbouzid MEH, Diallo D. Electric motor drive selection issues for  
39  
40 HEV propulsion systems: A comparative study. IEEE Trans Veh Technol  
41  
42 2006;55(6):1756-64.  
43  
44  
45

46 [19] Ruan J, Walker PD, Wu J, Zhang N, Zhang B. Development of continuously  
47  
48 variable transmission and multi-speed dual-clutch transmission for pure electric vehicle.  
49  
50 Adv Mech Eng 2018;10(2):1687814018758223.  
51  
52  
53  
54  
55  
56  
57  
58  
59  
60  
61  
62  
63  
64  
65

- 
- 1 [20] Ming Z. A computationally intelligent methodologies and sliding mode control  
2 based traction control system for in-wheel driven EV. In: 2006 CES/IEEE 5th  
3 International Power Electronics and Motion Control Conference, vol. 2; 2006. p. 1-5.  
4  
5  
6  
7  
8  
9 [21] Ji FZ, Xu LC, Wu ZX. Effect of driving cycles on energy efficiency of electric  
10 vehicles. *Sci China Ser E* 2009;52(11):3168.  
11  
12  
13 [22] Rahman Z, Ehsani M, Butler KL. An investigation of electric motor drive  
14 characteristics for EV and HEV propulsion systems. *SAE trans* 2000;2396-403.  
15  
16  
17 [23] Akehurst S, Vaughan ND, Parker DA, Simner D. Modeling of loss mechanisms in  
18 a pushing metal V-belt continuously variable transmission, part 1: torque losses due to  
19 band friction. *Proc Inst Mech Eng Part D* 2004;218(11):1269-81.  
20  
21  
22 [24] Akehurst S, Vaughan ND, Parker DA, Simner D. Modeling of loss mechanisms in  
23 a pushing metal V-belt continuously variable transmission, part 2: pulley deflection  
24 losses and total torque loss validation. *Proc Inst Mech Eng Part D* 2004;218(11):1283-  
25 93.  
26  
27  
28 [25] Akehurst S, Vaughan ND, Parker DA, Simner D. Modeling of loss mechanisms in  
29 a pushing metal V-belt continuously variable transmission, part 3: belt slip losses. *Proc*  
30 *Inst Mech Eng Part D* 2004;218(11):1295-306.  
31  
32  
33 [26] Ruan J, Walker P, Zhang N. A comparative study energy consumption and costs of  
34 battery electric vehicle transmissions. *Appl Energy* 2016;165:119-34.  
35  
36  
37 [27] Hu J, Mei B, Peng H, Guo Z. Discretely variable speed ratio control strategy for  
38 continuously variable transmission system considering hydraulic energy loss. *Energy*  
39 2019;180:714-27.  
40  
41  
42  
43  
44  
45  
46  
47  
48  
49  
50  
51  
52  
53  
54  
55  
56  
57  
58  
59  
60  
61  
62  
63  
64  
65

---

1 [28] Kwon K, Seo M, Min S. Efficient multi-objective optimization of gear ratios and  
2  
3 motor torque distribution for electric vehicles with two-motor and two-speed  
4  
5 powertrain system. *Appl Energy* 2020;259:114190.  
6  
7

8  
9 [29] Pareschi G, Küng L, Georges G, Boulouchos K. Are travel surveys a good basis  
10  
11 for EV models? Validation of simulated charging profiles against empirical data. *Appl*  
12  
13 *Energy* 2020;275:115318.  
14  
15

16  
17 [30] Zhuang W, Li S, Zhang X, Kum D, Ju F. A survey of powertrain configuration  
18  
19 studies on hybrid electric vehicles. *Appl Energy*, 2020;262:114553.  
20  
21

22  
23 [31] Araque ES, Colin G, Cloarec GM, Ketfi-Cherif A, Chamaillard Y. Energy analysis  
24  
25 of eco-driving maneuvers on electric vehicles. *IFAC-PapersOnLine* 2018;51(31):195-  
26  
27 200.  
28  
29

30  
31 [32] Okada T, Kumano K, Okuda Y, Tashiro N, Imanishi Y, Iihoshi Y. Powertrain  
32  
33 Systems Improving Real-world Fuel Economy. *Hitachi Rev* 67(1):122-123.  
34  
35

36  
37 [33] Kato H, Ando R, Kondo Y, Suzuki T, Matsushashi K, Kobayashi S. Comparative  
38  
39 measurements of the eco-driving effect between electric and internal combustion  
40  
41 engine vehicles. In: 2013 World Electric Vehicle Symposium and Exhibition, IEEE;  
42  
43 2013. p. 1-5.  
44  
45

46  
47 [34] Koch A, Bürchner T, Herrmann T, Lienkamp M. Eco-Driving for Different Electric  
48  
49 Powertrain Topologies Considering Motor Efficiency. *World Electr Veh J* 2021:12(1):6.  
50  
51

52  
53 [35] Sayed K, Kassem A, Saleeb H, Alghamdi AS, Abo-Khalil AG. Energy-Saving of  
54  
55 Battery Electric Vehicle Powertrain and Efficiency Improvement during Different  
56  
57 Standard Driving Cycles. *Sustainability* 2020:12(24):10466.  
58  
59  
60  
61

- 
- 1 [36] Zheng H, Wu J, Wu W, Zhang Y, Huang YS. Eco-driving of electric vehicles with  
2 integrated motion and battery dynamics. In: 2019 IEEE 16th International Conference  
3 on Networking, Sensing and Control; 2019. p. 299-304.  
4  
5  
6  
7  
8  
9 [37] Chen Y, Rozkvas N, Lazar M. Driving Mode Optimization for Hybrid Trucks  
10 Using Road and Traffic Preview Data. *Energies*, 2020;13(20):5341.  
11  
12  
13  
14 [38] Wang G, Makino K, Harmandayan A, Wu X. Eco-driving behaviors of electric  
15 vehicle users: A survey study. *Transp Res Part D* 2020;78:102188.  
16  
17  
18  
19 [39] Ehsani M, Gao Y, Longo S, Ebrahimi K. Modern electric, hybrid electric, and fuel  
20 cell vehicles. CRC press 2018.  
21  
22  
23  
24  
25 [40] Li SE, Peng H. Strategies to minimize the fuel consumption of passenger cars  
26 during car-following scenarios. *Proc Inst Mech Eng Part D* 2012;226(3):419-29.  
27  
28  
29  
30 [41] Wu J, Wei Z, Li W, Wang Y, Li Y, Sauer UD. Battery thermal-and health-  
31 constrained energy management for hybrid electric bus based on soft actor-critic DRL  
32 algorithm. *IEEE Trans. Ind. Inform* 2020;17(6):3751-61.  
33  
34  
35  
36  
37  
38 [42] Xu R. The research on design and performance simulation of dynamic system of  
39 electric postal car. Wuhan University of technology, China: 2013.  
40  
41  
42  
43 [43] Vu H, Shin D. Scheduled pre-heating of Li-Ion battery packs for balanced  
44 temperature and state-of-charge distribution. *Energies* 2020;13(9):2212.  
45  
46  
47  
48  
49 [44] Coleman M, Zhu CB, Lee CK, Hurley WG. A combined SOC estimation method  
50 under varied ambient temperature for a lead-acid battery. In: Twentieth Annual IEEE  
51 Applied Power Electronics Conference and Exposition, 2005; 2005. p. 991-7.  
52  
53  
54  
55  
56  
57  
58  
59  
60  
61  
62  
63  
64  
65

---

1 [45] Bernardi D, Pawlikowski E, Newman J. A general energy balance for battery  
2 systems. *J Electrochem Soc* 1985;132(1):5-12.  
3  
4  
5  
6 [46] Hou Y, Sai Y, Meng L, Shi J. Modeling and simulation of thermal effects of  
7 lithium-ion battery for electric vehicles. *Chinese J. Power Sources* 2016;40(6):1185-8.  
8  
9  
10  
11 [47] Wang R, Lukic SM. Dynamic programming technique in hybrid electric vehicle  
12 optimization. In: 2012 IEEE International Electric Vehicle Conference; 2012. p. 1-8.  
13  
14  
15  
16 [48] Chen BC, Wu YY, Tsai HC. Design and analysis of power management strategy  
17 for range extended electric vehicle using dynamic programming. *Appl Energy*  
18 2014;113:1764-74.  
19  
20  
21  
22  
23  
24  
25 [49] Asher ZD, Baker DA, Bradley TH. Prediction error applied to hybrid electric  
26 vehicle optimal fuel economy. *IEEE Trans Control Syst Technol* 2017;26(6):2121-34.  
27  
28  
29  
30  
31  
32  
33  
34  
35  
36  
37  
38  
39  
40  
41  
42  
43  
44  
45  
46  
47  
48  
49  
50  
51  
52  
53  
54  
55  
56  
57  
58  
59  
60  
61  
62  
63  
64  
65